FEDERAL UNIVERSITY OF SANTA CATARINA

TECHNOLOGICAL CENTER

GRADUATE PROGRAM IN CHEMICAL ENGINEERING

Felipe Pereira da Costa

DEVELOPMENT OF AN ENZYMATIC BIOSENSOR USING ORGANIC-INORGANIC HYBRIDS FOR DETECTION OF PHENOL

FLORIANÓPOLIS

2021

Felipe Pereira da Costa

DEVELOPMENT OF AN ENZYMATIC BIOSENSOR USING ORGANIC-INORGANIC HYBRIDS FOR DETECTION OF PHENOL

Master thesis as a requirement for obtaining a master's degree in Chemical Engineering presented to the Graduate Program in Chemical Engineering at the Federal University of Santa Catarina

Advisor: Prof. Agenor Furigo Junior, Dr.

Co-advisor: Rosana Oliveira Henriques, Dr.

FLORIANÓPOLIS

2021

Felipe Pereira da Costa

Development of an enzymatic biosensor using organic-inorganic hybrids for detection of phenol

The present work at master level was evaluated and approved by an examining board composed of the following members:

Prof. Agenor Furigo Junior, Dr.
Universidade Federal de Santa Catarina

Prof. Débora de Oliveira, Dr.
Universidade Federal de Santa Catarina

Prof. Jaciane Lutz Ienczak, Dr.
Universidade Federal de Santa Catarina

We certify that this is the original and final version of the final paper wich was deemed appropriate to obtain the title of Master in Chemical Engineering.

————————————————————

Prof. Débora de Oliveira, Dr.
Coordinator of the Graduate Program in Chemical Engineering
Universidade Federal de Santa Catarina

————————————————————

Prof. Agenor Furigo Junior, Dr.
Advisor
Universidade Federal de Santa Catarina

Florianópolis, 2021.

ACKNOWLEDGEMENTS

RESUMO

Fenol, um poluente ambiental frequentemente encontrado em efluentes de indústrias químicas, é altamente tóxico mesmo em baixas concentrações. O presente estudo relata um método simples, rápido e de baixo impacto ambiental para biodetecção visual qualitativa de fenol usando nanoflores híbridas orgânico-inorgânicas de enzima *horseradish peroxidase* (HRP) com íons de cobre (Cu^{2+}-hNF) e de cálcio (Ca^{2+}-hNF). A enzima foi imobilizada pela técnica de automontagem da proteína em híbridos orgânico-inorgânicos, que na sequência foram suportados na superfície de uma membrana de fluoreto de polivinilideno (PVDF). A eficiência da imobilização da enzima em estruturas híbridas foi comprovada pelas técnicas de microscopia eletrônica de varredura (MEV), espectroscopia de energia dispersiva de raios-X (EDX), espectroscopia de infravermelho com transformada de Fourier (FTIR) e difração de raios-X (XRD). A melhor concentração de proteína na síntese dos híbridos foi determinada como 0,25 mg.mL^{-1} para ambos os íons metálicos. A melhor temperatura e o melhor pH de uso encontrados foram 60 °C e 7,4, respectivamente, tanto para os híbridos quanto para a enzima livre, sugerindo que a imobilização não afetou as condições ótimas da HRP livre. A estabilidade térmica de 25 °C a 70 ºC e a estabilidade em pH de 4,0 a 9,0 dos híbridos também foram determinadas. Finalmente, ambos os biossensores produzidos em membrana de PVDF, usando híbridos de cobre e cálcio, foram capazes de detectar fenol em concentrações variando de 0,72 µmol.mL^{-1} a 24,00 µmol.mL^{-1} em 1 min de reação, enquanto biossensores de controle produzidos com quantidade equivalente de enzima livre não apresentaram mudança de cor perceptível nas mesmas condições. Os resultados sugerem uma aplicação promissora dos biossensores desenvolvidos na detecção de fenol.

Palavras-chave: Biossensores. Híbridos orgânico-inorgânicos. Imobilização enzimática. Horseradish peroxidase.

RESUMO EXPANDIDO

Introdução

Primeiramente descrita por Ge, Lei e Zare (2012), a síntese de híbridos orgânico-inorgânicos como forma de imobilização enzimática sem suporte têm recebido crescente interesse de pesquisa na área de biocatálise (GE; LEI; ZARE, 2012; BILAL *et al.*, 2019). Um dos motivos está relacionado à simplicidade de síntese dessas estruturas, também conhecidas como *nanoflowers* por conta de seu formato característico, que necessita apenas da presença de enzima, íons fosfato e íons metálicos, em condições brandas, como temperatura ambiente e pressão atmosférica (BATULE *et al.*, 2019). Outra razão se refere à melhoria das propriedades dos biocatalisadores frente aos métodos tradicionais de imobilização, como alta área superficial, aumento da estabilidade e excelente atividade catalítica (PARK *et al.*, 2017; YE *et al.*, 2016). À vista disso, a aplicação de *nanoflowers* híbridas é observada em diferentes áreas como biossíntese e biodegradação de compostos e na produção de biossensores (WANG *et al.*, 2020; LUO *et al.*, 2020; CHEON *et al.*, 2019). Fenol tem sido frequentemente utilizado como alvo de biossensores enzimáticos, devido a sua alta toxicidade e incidência recorrente em efluentes de diversas indústrias químicas, como papel e celulose, refinaria de petróleo, farmacêutica, e de revestimento metálico (GAY *et al.*, 2020; JUN *et al.*, 2019). Diferentes enzimas podem ser usadas para este propósito, como tirosinases, lacases e peroxidases (WEN *et al.*, 2020; OTHMAN *et al.*, 2020; RAHEMI *et al.*, 2019). Contudo, muitas vezes a produção de tais biossensores envolve uma ou mais técnicas complexas. Sob essa perspectiva, este trabalho pretendeu desenvolver um biossensor rápido, prático e eficiente para fenol utilizando estruturas híbridas orgânico-inorgânicas de enzima *horseradish peroxidase* (HRP) e íons de cobre e cálcio.

Objetivos

O objetivo geral deste trabalho foi desenvolver um biossensor colorimétrico para detecção de fenol usando estruturas híbridas orgânico-inorgânicas do tipo *nanoflower* de enzima HRP e íons de cobre e cálcio. Os objetivos específicos compreenderam a síntese e caracterização química, estrutural e catalítica dos híbridos, bem como a avaliação da eficiência de detecção de fenol do biossensor produzido.

Metodologia

Inicialmente, a melhor concentração de enzima na síntese dos híbridos foi avaliada da seguinte forma: 67 µL de uma solução de $CuSO_4$ 120 mM foram adicionados a 10 mL de soluções de HRP (Toyobo, Brasil) em diferentes concentrações (0,1; 0,25; 0,5; 1,0 mg.mL^{-1}) em tampão fosfato 100 mM, pH 7,4 e 0,1% de NaCl. A mistura foi agitada por 30 s em vórtex e em seguida incubada por 72 h a 4 °C. Híbridos de cálcio e HRP foram feitos com a melhor condição encontrada nos híbridos de cobre, usando 67 µL de $CaCl_2$ 120 mM. As *nanoflowers* produzidas foram coletadas por centrifugação a 4000 rpm por 15 min. As estruturas híbridas foram caracterizadas por microscopia eletrônica de varredura (MEV), espectroscopia de raios-X por dispersão de energia (EDS), espectroscopia de infravermelho com transformada de Fourier

(FTIR) e difração de raios-X (XRD). Os testes de atividade e determinação de velocidade inicial de reação foram realizados com base na formação de quinoneimina, um composto cromóforo que pode ser quantificado por espectrofotometria. Para esta finalidade, 1.5 mL de H_2O_2 0.0017 M em tampão fosfato 0.2 M e pH 7.4 foram misturados com 1.4 mL de uma solução contendo 0.17 M de fenol e 0.0025 M de 4-aminoantipirina (4-AAP). A reação foi iniciada com a adição de 0.1 mL de uma suspensão de *nanoflowers* ou enzima HRP e medida em espectrofotômetro a 510 nm em 1 min e 25 ºC. A eficiência de imobilização foi determinada para concentrações iniciais de enzima de 0,1; 0,25 e 0,5 mg.mL^{-1}, para ambos os íons de cobre e de cálcio, com base na atividade do sobrenadante após formação dos híbridos e centrifugação do meio, comparando-se com a atividade enzimática inicial anterior à adição dos íons metálicos. As melhores condições de uso da enzima livre e suas formas imobilizadas foram determinadas aplicando-se o método anteriormente descrito, variando-se o pH do meio de 3,0 a 13,0 e a temperatura de reação de 25 °C a 70 °C. A estabilidade enzimática foi avaliada de forma análoga, em pH de 4,0 a 9,0 e nas temperaturas 50 °C, 60 °C e 70 °C. Em seguida, foram determinados os parâmetros cinéticos K_M e V_{max} do modelo de Michaelis-Menten para reações enzimáticas simples, utilizando fenol como substrato. Da mesma forma, foi avaliado o número de renovação, ou k_{cat}, com base na velocidade inicial específica de reação. A determinação dos parâmetros cinéticos específicos teve como finalidade a comparação quantitativa da eficiência da enzima livre e de suas formas imobilizadas. Finalmente, foram produzidos os biossensores da seguinte maneira: 10 µL da suspensão de *nanoflowers* foram depositados na superfície de uma membrana de fluoreto de polivinilideno de 1 cm^2, com diâmetro de poro de 0.22 µm, que foram deixados para secar por 12 horas a temperatura ambiente. Os biossensores foram então testados utilizando-se 50 µL de uma solução contendo H_2O_2 0,88 µmol.mL^{-1}, 4-AAP 1,1 µmol.mL^{-1} e fenol com concentrações entre 0,72 µmol.mL^{-1} e 24,00 µmol.mL^{-1} em tampão fosfato 0,2 M e pH 7,4. A presença de fenol em solução seria evidenciada pela mudança de coloração do biossensor em 1 min de reação.

Resultados e Discussão

O efeito da concentração enzimática na formação dos híbridos de cobre foi avaliado por análises de MEV. A melhor concentração inicial encontrada foi de 0,25 mg.mL^{-1}, com base na melhor formação estrutural dos híbridos, considerando-se bom tamanho e boa uniformidade. Esta foi, portanto, a concentração escolhida para síntese das estruturas híbridas de cálcio e enzima HRP. Contudo, os híbridos de cálcio feitos nas mesmas condições não apresentaram uma forma definida, mostrando que além da concentração de enzima, o tipo de íon utilizado está diretamente relacionado com a estrutura dos híbridos produzidos. Os testes de eficiência de imobilização indicaram que a melhor concentração enzimática na síntese das *nanoflowers* foi de 0,25 mg.mL^{-1} para ambos os íons, levando a uma eficiência de 92,3% para os híbridos de cobre, e 92,0% para os híbridos de cálcio. As análises de EDS indicaram uma correta formação química das *nanoflowers*, apresentando os picos referentes aos elementos característicos e esperados C, O e P em ambas as estruturas, além de Cu e Ca nos respectivos híbridos. A análise de FTIR foi utilizada para identificar as estruturas químicas dos híbridos. Picos referentes a estrutura da enzima HRP e aos fosfatos associados à formação dos híbridos foram verificados em ambas as amostras. Com a análise de XRD, foi possível identificar que os híbridos de HRP e cobre eram formados por cristais de $Cu_3(PO_4)_2 \cdot 3H_2O$ (JCPDS No. 00-022-0548), enquanto o

espectro dos híbridos de cálcio apresentou consistência de picos com $Ca_3(PO_4)_2 \cdot 2H_2O$ (JCPDS No. 18-0303) e $CaHPO_4$ (JCPDS No. 9-80). Analisando-se a atividade enzimática em diferentes valores de pH, constatou-se que o melhor pH reacional para ambos os híbridos, assim como para a enzima, livre foi de 7,4. Utilizando o melhor valor de pH, foram determinadas as atividades em função da temperatura de reação. A melhor temperatura foi, analogamente, definida como 60 °C para todas as formas do biocatalisador. Ambos os resultados estão de acordo com o que foi reportado previamente na literatura, onde a formação de híbridos orgânico-inorgânicos não levou a uma alteração nas melhores condições de uso da enzima (RONG *et al.*, 2017; MEMON *et al.*, 2019; SUN *et al.*, 2014; WANG *et al.*, 2020). Também foi observado que os híbridos de cálcio apresentaram maior atividade relativa em todas as temperaturas, quando comparados à enzima livre e aos híbridos de cobre. Referente à estabilidade, em valores de pH entre 6,0 e 9,0, tanto a enzima livre quanto os híbridos de cobre e de cálcio apresentaram perfis semelhantes de atividade relativa em função do tempo em até 8 horas. Entretanto, em meios ácidos de pH 4,0 e 5,0, foi notável uma maior desativação dos híbridos de cálcio em comparação com as outras formas do biocatalisador, sugerindo que a estabilidade dos híbridos esteja diretamente relacionada tanto com sua porção orgânica quanto sua porção inorgânica. A análise de estabilidade térmica mostrou excelente estabilidade dos híbridos e da enzima livre a 50 °C, sem que houvesse uma perda de atividade considerável durante as 8 horas de teste. A 60 °C, as atividades residuais observadas em 8 horas foram de 79,61%; 76,61%; e 74,97% referentes às atividades iniciais da enzima livre, dos híbridos de cobre e dos híbridos de cálcio, respectivamente. A 70 °C, foi notado o efeito favorável da imobilização enzimática em híbridos de cálcio. Enquanto a enzima livre perdeu toda a atividade em 6 horas, e os híbridos de cobrem apresentavam apenas 5,59% de atividade residual, os híbridos de cálcio mantiveram 27,02% da atividade inicial no mesmo tempo. O resultado sugere uma maior estabilidade térmica nos híbridos de enzima e cálcio, em conformidade ao que foi previamente descrito na bibliografia (DUAN; LI; ZHANG, 2018; CHEN *et al.*, 2018). Apesar de a reação estudada ter um mecanismo complexo, nas condições testadas a taxa observada de reação é função da concentração de fenol, indicando que essa é a etapa lenta do mecanismo e determinante da velocidade. A constante de Michaelis, K_M, está associada à afinidade entre o sítio ativo da enzima e o substrato, sendo que menores valores da constante representam maior afinidade. Neste sentido, observou-se que a imobilização da enzima em *nanoflowers* levou a uma diminuição do K_M, de 6,82 $\mu mol.mL^{-1}$ na enzima livre para 4,05 $\mu mol.mL^{-1}$ nos híbridos de cobre e 2,84 $\mu mol.mL^{-1}$ nos híbridos de cálcio, indicando maior afinidade sítio ativo–substrato nas estruturas híbridas, sobretudo nas de cálcio. A velocidade máxima específica de reação, contudo, não sofreu alteração considerável para as estruturas de cálcio e diminuiu para as estruturas de cobre. A pesquisa anterior de Zhong *et al.* (2021) corrobora o resultado, já que os híbridos orgânico-inorgânicos produzidos pelos autores apresentam ambos K_M e V_{max} menores que os da enzima livre, evidenciando que uma maior afinidade sítio ativo-substrato não necessariamente leva a uma maior velocidade de reação. O parâmetro k_{cat} permaneceu semelhante ao da enzima livre nos híbridos de cálcio e diminuiu consideravelmente para os híbridos de cobre. Os híbridos de cálcio destacaram-se ao apresentar um valor de k_{cat}/K_M, que representa a eficiência catalítica, cerca de 2,23 vezes maior que da enzima livre. Este resultado sugere que a imobilização da enzima HRP em híbridos orgânico-inorgânicos feitos a partir de íons de cálcio possa levar a uma maior eficiência enzimática. Similarmente, Zhang *et al.* (2020)

relataram uma eficiência catalítica maior para híbridos de cálcio e menor para híbridos de cobre, quando comparados à enzima livre. Finalmente, os biossensores produzidos foram testados com amostras contendo fenol em concentrações de 0,72 µmol.mL^{-1} a 24,00 µmol.mL^{-1}. Os biossensores com híbridos de cobre e de cálcio apresentaram coloração semelhante em 1 min de reação em todos os pontos testados, comprovando sua eficiência na rápida detecção de fenol. Em concentrações de fenol abaixo de 0,72 µmol.mL^{-1}, nenhum foi capaz de apresentar mudança de coloração que identificasse a presença do composto em 1 min. Os biossensores produzidos com quantidade equivalente de enzima livre não apresentaram resposta colorimétrica à solução fenólica testada. Acredita-se que isso tenha ocorrido devido ao espalhamento da enzima não imobilizada pelos poros da membrana. Uma síntese típica de *nanoflowers* utilizando o método descrito utiliza apenas 2,5 mg de enzima HRP e é capaz de gerar até 200 unidades de detecção para fenol, evidenciando uma abordagem prática e simples para produção de biossensores colorimétricos qualitativos para fenol em concentrações a partir de 0,72 µmol.mL^{-1}.

Conclusões

A produção de biossensores colorimétricos em membrana utilizando híbridos orgânico-inorgânicos de enzima HRP e íons de cobre e cálcio para detecção de fenol foi bem-sucedida. Ambos os biossensores, desenvolvidos com *nanoflowers* de diferentes íons metálicos, foram capazes de detectar fenol em concentrações de 0,72 µmol.mL^{-1} a 24,00 µmol.mL^{-1} em apenas 1 min de reação. Biossensores controle, produzidos com quantidade equivalente de enzima livre, não apresentaram mudança de cor nas mesmas condições. A correta formação dos híbridos foi verificada através das técnicas EDS, FTIR e XRD, apesar da divergência estrutural observada em MEV nos híbridos de cálcio em comparação com os híbridos de cobre. Os híbridos mostraram excelente estabilidade em função de pH e temperatura, especialmente os de cálcio, que foram capazes de manter a atividade por maior tempo em 70 °C. Além disso, os parâmetros cinéticos indicaram uma maior eficiência catalítica nos híbridos de cálcio do que na enzima livre. Os resultados obtidos sugerem uma próspera aplicação de híbridos orgânico-inorgânicos na produção de biossensores colorimétricos para detecção de fenol.

Palavras-chave: Híbridos orgânico-inorgânicos. Nanoflores híbridas. Imobilização enzimática. Horseradish peroxidase. Detecção de fenol.
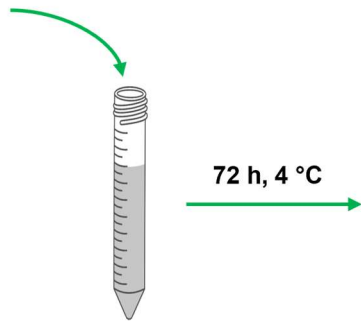
ABSTRACT

Phenol, an environmental pollutant frequently found in chemical industries effluents, is highly toxic even in low concentrations. This study reports a green, simple, and rapid method for visual qualitative phenol biosensing using horseradish peroxidase (HRP) hybrid nanoflowers made with copper (Cu^{2+}-hNF) and calcium (Ca^{2+}-hNF) ions. The enzyme was immobilized through protein-inorganic self-assembly into hybrid structures, subsequently supported onto a polyvinylidene fluoride (PVDF) membrane. The effective enzyme encapsulation into hybrid structures was sustained by scanning electron microscopy (SEM), energy-dispersive X-ray spectroscopy (EDS), Fourier transform infrared spectroscopy (FTIR), and powdered X-ray diffraction (XRD) techniques. The best protein concentration in hybrid synthesis was established as 0.25 mg.mL^{-1} for both metal ions. The best temperature and pH of use were found to be 60 °C and 7.4, respectively, for both hybrids and the free enzyme, suggesting that the immobilization did not affect the optimal conditions of the free HRP. Thermal stability from 25 °C to 70 ºC and pH stability from 4.0 to 9.0 of the hybrids were also determined. Finally, using copper and calcium hybrids, both biosensors produced onto a PVDF membrane could detect phenol in concentrations ranging from 0.72 µmol.mL^{-1} to 24.00 µmol.mL^{-1} within 1 min, whereas control biosensors produced with an equivalent amount of free enzyme have not presented a visible color change in the same conditions. The findings suggest a promising application of the developed biosensors in functional phenol detection.

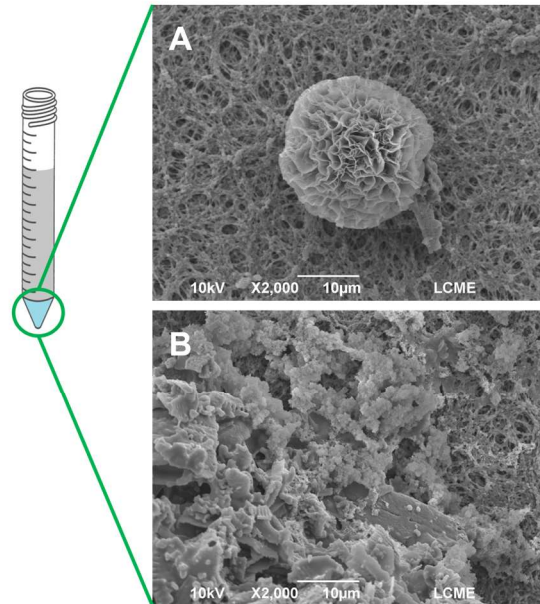**Keywords**: Organic-inorganic hybrids. Hybrid nanoflowers. Enzyme immobilization. Horseradish peroxidase.

GRAPHICAL ABSTRACT

(A) Cu^{2+} or (B) Ca^{2+} 0.8 mM

72 h, 4 °C
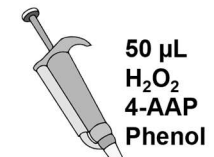
HRP 0.25 mg.mL^{-1}
PBS 0.1 M, pH 7.4

10 μL

PVDF
membrane

12 h, 25 °C

50 μL
H$_2$O$_2$
4-AAP
Phenol

1 min

$2\,H_2O_2 + $ phenol $ + $ 4-AAP $\xrightarrow{\text{peroxidase}}$ product $ + 4\,H_2O$

INDEX OF FIGURES

INDEX OF TABLES

LIST OF ABBREVIATIONS AND ACRONYMS

hNF	Hybrid nanoflowers
HRP	Horseradish peroxidase
SEM	Scanning electron microscopy
EDS	Energy dispersive X-ray spectroscopy
FTIR	Fourier transform infrared spectroscopy
XRD	Powdered X-ray diffraction
BSA	Bovine serum albumin
TEM	Transmission electron microscopy
XPS	X-ray photoelectron spectroscopy
DSC	Differential scanning calorimetry
PPL	Porcine pancreas lipase
GOx	Glucose oxidase
PVA-co-PE	Poly(vinyl alcohol-co-ethylene)
PMMA	Poly(methyl methacrylate)
4-AAP	4-aminoantipyrine
MNPs	Magnetic nanoparticles
AUR	Amplex UltraRed
CFU	Colony forming unit
EU	European Union
USEPA	United States Environmental Protection Agency
PVDF	Polyvinylidene fluoride
PBS	Phosphate buffered saline
rpm	Revolutions per minute
Cu^{2+}-hNF	Copper-HRP hybrid nanoflowers
Ca^{2+}-hNF	Calcium-HRP hybrid nanoflowers
a.u.	Arbitrary unit
AKR	Aldo-keto reductase
ADH	Alcohol dehydrogenase
LOD	Limit of detection

LIST OF SYMBOLS

A	Enzymatic activity ($U.L^{-1}$)
ΔAbs	Absorbance variance (a.u.)
t	Time (s)
ε	Molar absortion coefficient ($L.mmol^{-1}.cm^{-1}$)
b	Light path length (cm)
Y	Encapsulation yield (%)
A_i	Initial activity (U)
A_s	Activity of the supernatant after immobilization (U)
V_0	Initial specific reaction rate ($\mu mol.min^{-1}.mg^{-1}$)
C_E	Enzyme concentration ($mg.mL^{-1}$)
K_M	Michaelis constant ($\mu mol.mL^{-1}$)
V_{max}	Maximum specific reaction rate ($\mu mol.min^{-1}.mg^{-1}$)
k_{cat}	Catalytic constant (s^{-1})
k_{cat}/K_M	Catalytic efficiency ($s^{-1}.mM^{-1}$)

SUMMARY

1 INTRODUCTION

Peroxidases (EC 1.11.1.x) encompass a vast group of valuable biocatalysts involved in the numerous oxidative reactions which use peroxide as an electron acceptor. They perform an essential function in many biologic reactions in almost all living organisms. Consequently, it is not difficult to find peroxidases with distinct origins being employed in the most diverse scenarios, such as food engineering [1–3], pharmaceutical applications [4,5], and wastewater treatment [6–10]. Among those, horseradish peroxidase (HRP, EC 1.11.1.7) represents the principal source of commercial peroxidases [11].

Despite all sources of peroxidases and the relative facility to obtain them, enzyme immobilization is needed to ensure superior stability, facilitated recovery, and consequent re-usability [12]. However, traditional immobilization techniques tend to cause a decrease in enzyme activity, which might represent additional costs to the process. Against this background, organic-inorganic hybrid nanoflowers are one of the most recent and facile immobilization approaches, that enables improved stability and higher activities in immobilized enzymes compared to their free forms [13]. Since the first report of their synthesis, organic-inorganic hybrids have been broadly employed in diverse applications, like bioremediation [14–17] and synthetic chemicals production [18–20]. Nevertheless, the main application of hybrid nanoflowers has been in biosensors development [21–26].

Enzymatic biosensors have been widely used to detect phenol due to their high toxicity and recurrent incidence in effluents of many chemical industries, such as paper and cellulose, petroleum refining, pharmaceutical, and metal coating [27,28]. Different enzymes are employed for this purpose, like tyrosinase [29–34], laccase [35–39], and peroxidase [40–46]. However, those biosensors often exploit interwoven elaborated techniques, which might portray a barrier to *in situ* phenol analysis as an environmental pollutant.

Hence, the main idea of this research was to develop a simple, rapid, and low-cost biosensor for visual phenol detection by employing HRP-inorganic hybrid nanoflowers. Furthermore, this work investigates the differences between copper and calcium hybrids by applying various structural, chemical, and catalytic characterization techniques.

1.1 OBJECTIVES

1.1.1 General objective

The general objective of this work was to develop a colorimetric membrane-based biosensor for phenol detection using copper/calcium–horseradish peroxidase hybrid nanoflowers.

1.1.2 Specific objectives

- To synthesize hybrid nanoflowers of copper and calcium ions and horseradish peroxidase enzyme.
- To examine the influence of protein concentration and metal ion type in nanoflowers synthesis.
- To verify the proper formation of hybrid nanoflowers through scanning electron microscopy (SEM), energy-dispersive X-ray spectroscopy (EDS), Fourier transform infrared spectroscopy (FTIR), and powdered X-ray diffraction (XRD).
- To determine the best operating conditions of temperature and pH of copper and calcium hybrids and the free enzyme.
- To assess pH and thermal stability of copper and calcium hybrids and the free enzyme.
- To estimate the kinetic parameters of copper and calcium hybrids and the free enzyme.
- To produce a biosensor by supporting the hybrid nanoflowers onto a polyvinylidene fluoride (PVDF) membrane.
- To evaluate the efficiency of the developed biosensors in phenol detecting.

2 LITERATURE REVIEW

Enzymes have their great potential recognized and established in various industrial sectors, such as food, drug, and fuel production for many years [47–49]. Due to these biocatalysts' versatility and advantages over chemical catalysts, such as milder operating conditions, their research and application are constantly growing [50]. The use of enzymes tends to minimize industrial production costs by reducing energy consumption and by-products formation due to the high specificity of the biocatalyst and reducing the amount of waste generated in the process [51]. Nevertheless, there are some limitations to using enzymes on a large scale, such as the biocatalyst's high cost and its low stability under extreme reaction conditions [52].

As an alternative to solve these problems, different immobilization techniques are applied to improve the enzyme stability, specificity, selectivity, ease of recovery, and reuse [53,54]. However, most standard immobilization techniques lead to significant losses of biocatalyst activity compared to its free form, lower reaction rates, and additional process costs related to immobilization [47].

Due to some obstacles faced by the application of immobilized enzymes at and industrial level, new enzyme immobilization techniques were emerging. To improve the surface area and stability of biocatalysts, researchers developed flower-shaped nanostructures. In this process, layers of organic-inorganic hybrid structures are formed, such as the flower petals, they are thus called *nanoflowers* [55–57]. Although inorganic nanoflowers have their applications in catalysis and analytical sciences researched since the beginning of the century, organic-inorganic structures have gained a greater interest in recent years in biocatalysis with growing research efforts [13,58]. These structures are formed by an inorganic part composed of a metal phosphate and an organic part composed of DNA molecules or proteins, such as enzymes [23]. Among the advantages of these nanomaterials compared to the traditional immobilization methods are high surface area, simplicity of synthesis, higher stability, and excellent catalytic activity [59,60]. These features enable and encourage the application of hybrid nanoflowers in various areas, such as biomedicine, biocatalysis, and the development of biosensors [59–63].

Different enzymes and approaches are used to produce biosensors. Among those, phenolic compounds are recurrently employed as targets due to their toxicity and habitual incidence in chemical industries effluents [27,28].

Given the above, the current chapter presents a literature review of organic-inorganic hybrid nanoflowers, their applications in several areas of enzymatic catalysis, and phenol as an environmental pollutant.

2.1 SYNTHESIS, CHARACTERIZATION, AND CLASSIFICATION OF HYBRID NANOFLOWERS

The first studies that refer to nanometric flower-type structures synthesized them by heatin silicon compounds at high temperatures [64,65]. Many types of materials were studied later, such as copper ions [66], gold [67,68], zinc [69], platinum [70], among others.

The first synthesis of organic-inorganic hybrid nanoflowers (hNF), as described by Ge, Lei, and Zare [13], happened by accident when 20 µl of 120 mM $CuSO_4$ solution was added to 3 mL of phosphate-buffered saline (PBS) solution containing 0.1 $mg.mL^{-1}$ bovine serum albumin (BSA) at pH 7.4 and 25 ° C. The mixture was stirred for about 30 s and then incubated at rest for three days. After this period, a bluish precipitate with porous and flower-like structures was observed. With this study, Ge, Lei, and Zare [13] proposed a mechanism of formation of nanoflower structures, outlined in Fig. 1. Based on the use of BSA and copper ions, the suggested mechanism consists of three steps: (1) nucleation and formation of primary crystals, (2) growth of crystals, and (3) formation of nanoflowers. In the Fig. 1, yellow spheres represent protein molecules. Initially, Cu^{2+} ions react with phosphate ions to form the first crystals. In the same stage, there is the formation of Cu^{2+} complexes with the enzyme. The following stages refer to the growth of these crystals and nanoflowers' subsequent formation [13].

Figure 1 - Hybrid nanoflowers forming mechanism
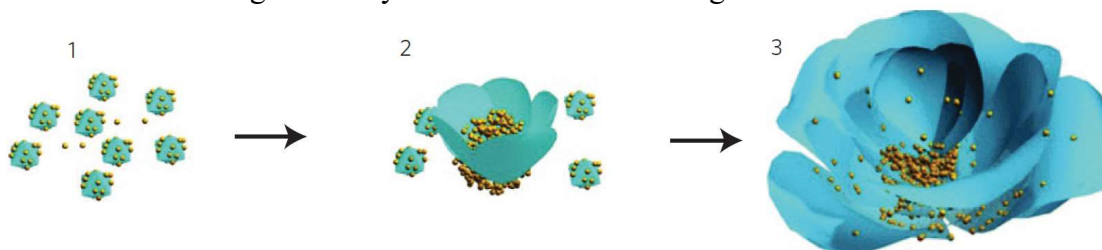
Source: Ge; Lei; Zare, 2012.

A similar mechanism is described by Kim *et al.* [71], who consider that the growth of hybrid nanoflowers can be divided into four stages: (1) initial nucleation and formation of an

enzyme/metal nanocomplex, (2) nanofiber self-assembly, (3) nano-hyperbranches formation and (4) final production of hybrid nanoflowers.

The search for structures with different characteristics for certain applications, such as optical, conductive, and mechanical features, guided the development of the area, especially concerning biosensors [70,72,73]. The hunt for materials and methods that can be used to immobilize enzymes united these areas, causing several studies to emerge with the use of nanoflowers in enzymatic processes.

To prove the generality of the described method, Ge, Lei and Zare, in their first study, replaced BSA by α-lactalbumin, laccase, carbonic anhydrase, and lipase, different enzymes, in different concentrations. The formation of hybrids was based on the coordination between Cu^{2+} ions and proteins, more specifically on the formation of complexes between the amino groups of the primary structure of enzymes with copper [74]. Similar structures to the initial nanoflowers were observed with different proteins used [13].

The simple formation of organic-inorganic hybrid nanoflowers depends on the incubation time, enzyme concentration, pH, and temperature. Several authors demonstrate the best formation of these structures, when more rounded and with more closed pores, allowing higher area/volume ratio, at temperatures of 4 °C, with a pH close to 7, and 72 h of incubation [13,55,71,75,76].

Considering the formation mechanisms described above, the number of nucleation points between metal ions and proteins decreases with enzyme concentration. Consequently, larger nanoflowers tend to be observed [13,77].

To decrease the synthesis time of the nanoflowers, some changes in the experimental conditions were suggested. The main one comprises the use of a sonicator bath, which can reduce the time formation of structures from 72 h to just a few minutes [78,79].

After the synthesis assays, it is necessary to characterize the structures and to confirm their proper formation. For this purpose, the reaction medium is centrifuged, allowing the separation of a precipitate where the generated nanoflowers are found.

Scanning electron microscopy (SEM) enables the morphological analysis of the nanoflower surface and the determination of its size. For the analysis of isolated nanoflowers and the crystalline structure of their petals, transmission electron microscopy (TEM) can be used. Previous reports show average structure sizes, depending on the type and concentration of the enzyme used, varying between 3 and 20 μm [13,42,80].

Determining the composition and the chemical interaction of the formed hybrids is also essential for the knowledge of the immobilized biocatalyst. Therefore, analyzes such as X-ray

excited photoelectron spectroscopy (XPS), X-ray diffraction (XRD), Fourier transform infrared spectroscopy (FTIR), differential scanning calorimetry (DSC), and energy-dispersive X-ray spectroscopy (EDS) can be applied [71,75,81].

Nanoflowers can be formed with different proteins or DNA, in addition to different metal ions. According to this, there is an attempt to classify these structures. Lee *et al.* [80] proposed classifying nanoflowers into five primary types: copper-protein, calcium-protein, manganese-protein, copper-DNA, and capsular nanoflowers.

Bilal *et al.* proposed a similar classification [82], taking into account the progress in research in the area. The authors classified the hybrids according to the metal ion used in the synthesis, the main types as being copper, calcium, manganese, zinc, cobalt, and iron nanoflowers.

Biocatalysts formed with flower-like structure proved to be efficient, stable and became excellent alternatives to "classic" immobilization processes that usually require solid supports. The efficiency and robustness of the "new" biocatalysts made them applicable in different industrial sectors, which will be discussed over the next topic of this work.

Classic immobilization processes typically include adsorption, covalent attachment, encapsulation, as well as another sophisticated combination of methods [83]. However, these methods may have some disadvantages, such as difficulties in the immobilitazion process, restriction in the enzyme's flexibility, impediments between enzyme and substrat, and blocks in the active site [55]. Therefore, the advent of nanoflowers might circumvent some of these disadvantages.

2.2 HYBRID NANOFLOWER APPLICATIONS IN BIOCATALYSIS

As a simple and elegant form of biocatalyst synthesis, the nanoflowers cab exhibit high stability and activity, improving mass transfers. Therefore, practical applications of organic-inorganic nanoflowers in diverse scenarios have received particular attention from researchers from all over the globe in the past few years. Table 1 summarizes their applications in three main categories: biosynthesis of chemicals, bioremediation and biodegradation of compounds, and biosensors production, individually examined in the following sections of this work.

Table 1 - Hybrid nanoflower applications in biocatalysis

(to be continued)

APPLICATION	METAL ION	ENZYME	REACTION	REFERENCE
Biosynthesis	calcium	lipase	synthesis of clindamycin palmitate	[18]
			synthesis of fructose ester	[19]
	copper		synthesis of biodiesel	[77]
		lipase + GOx	epoxidation of alkenes	[84]
		cytochrome P450*	oxidation of sulfides	[20]
		L-arabinitol 4-dehydrogenase + NADH oxidase	L-xylulose production	[85]
Bioremediation and Biodegradation	copper, cobalt, cadmium	chloroperoxidase	dye removal	[15]
	copper	peroxidase		[86]
		egg white*		[87]
		laccase + lysine		[14]
		laccase		[16] [17] [88]
			degradation of BPA	[89]
		trypsin	degradation of proteins	[90]
		papain	hydrolysis of proteins	[91]
	calcium	alkalase		[92]
	copper, manganese, zinc, cobalt, calcium	lactase	hydrolysis of lactose	[93]
Biosensors	manganese	GOx	glucose detection	[21]
	copper			[22] [23]
		GOx + HRP		[94] [95]

Table 1 - Hybrid nanoflower applications in biocatalysis

(conclusion)

APPLICATION	METAL ION	ENZYME	REACTION	REFERENCE
Biosensors	copper	HRP	phenol and hydrogen peroxide detection	[42]
		catalase	hydrogen peroxide detection	[24]
		laccase	phenol detection	[35]
			epinephrine detection	[78]
		lactoperoxidase	epinephrine and dopamine detection	[25]
		AChE + choline oxidase	organophosphorus pesticides detection	[96]
		CON A + hemin		[97]
		GOx + HRP	pathogens detection	[98]
	calcium	CON A + GOx		[26]

2.2.1 Biosynthesis of chemicals

Due to their excellent catalytic features, enzymes are used in a wide range of reactions. Among these, enzymatic synthesis reactions of esters gain prominence thanks to these compounds' versatility, whose applicability can be observed in the production from cosmetics to biofuels [99–101].

Using lipase ZC12 as the core of hybrid nanoflowers with calcium ions, Zhang *et al.* [19] demonstrated structures with a 206% increase in catalytic activity compared to the free enzyme. Also, an increase in selectivity at low temperatures was observed, and after 7 cycles of use, the immobilized lipase did not lose its activity. The authors finally tested the nanoflowers for the conversion of lauric acid into fructose ester, finding a conversion of 57% at 72 h and 40 °C, about 2 times greater than with lipase in its free form under the same conditions, proving the potential application of the hybrid structures [19].

Wang *et al.* [18] produced calcium phosphate and lipase hybrids aiming to synthesize clindamycin palmitate. Both ions Ca^{2+} and $(PO_4)^{3-}$ were obtained from animal bone waste. The authors have shown the efficiency of the hybrids produced even in high temperatures. In fact, at 80 °C, the reaction yield using the immobilized lipase was 52.6%, while no product was detected using the free enzyme.

Lipases can also be used for the synthesis of fatty acid esters, employed mainly in the biodiesel composition. Jiang *et al.* [77] used porcine pancreas lipase (PPL) with copper phosphate to form nanoflowers. The hybrids showed increased stability at high temperatures, leading to an increase in the reactions' efficiency.

Increasing the storage time is also a desirable feature when carrying out an enzymatic immobilization. This characteristic was observed by Jiang *et al.* [77], when lipase nanoflowers maintained 93.6% of their activity after 7 days of incubation at room temperature, while the free enzyme lost all its activity after about 48 h. Finally, the authors tested the hybrids formed for converting sunflower oil into biodiesel. The nanoflowers demonstrated higher resistance to the presence of methanol and low conversion loss after 5 cycles of the catalyst, from 96.5% to 72.5% [77].

The formation of organic-inorganic hybrid nanoflowers as an enzymatic immobilization technique allows more than one enzyme to be immobilized simultaneously in the same structure. The multifunctional biocatalysts can act in reactions that occur in multiple stages, either by eliminating one of them or assisting in eliminating undesirable by-products [102,103]. Zhang *et al.* [84] synthesized nanoflowers containing glucose oxidase (GOx) and lipase in the

presence of copper ions. The authors tested the use of the combined enzymes in the free form, immobilized separately and immobilized in the same structure for the epoxidation of styrene, with 51%, 65%, and 89% conversions, respectively. The results suggested a decrease in diffusion resistance and the concentration of hydrogen peroxide in the reaction medium, also reducing enzyme inactivation. After ten cycles, the co-immobilized enzymes' activity in the epoxidation reaction remained at 82%, proving the efficiency of reusing the biocatalyst [84].

Another application of hybrid structures was evaluated by He *et al.* [20] on the selective oxidation of sulfides. The authors produced nanoflowers from cytochrome P450, an extremely versatile biocatalyst for different reactions, and copper phosphate. This organic-inorganic hybrid was used in the oxidation of thioanisole into methyl phenyl sulfoxide. After five catalytic runs of 1 h at 35 °C, no significant decrease was observed in conversion and selectivity, which were higher than 93% and 99%, respectively.

2.2.2 Bioremediation and biodegradation of compounds

The degradation of compounds represents another widespread use of enzymes, as well as their immobilized forms. Enzymes are potent allies in the decomposition of complex molecules, such as drugs and dyes, in addition to enabling the hydrolysis of proteins since they can operate in mild operating conditions [104,105].

Different enzymes can decolorize synthetic and natural dyes, given the wide variety of compounds used as dyes and the versatility of biocatalysts. For example, copper and laccase hybrid nanoflowers can remove up to 90% color in solution [16,17,88]. Rong *et al.* [16] observed a removal rate of 3.6 times higher with nanoflowers than that of the free enzyme for Congo Red dye. Patel *et al.* [17] also synthesized laccase hybrids, but the nanoflowers were cross-linked with glutaraldehyde. This considerable change in the structure, illustrated in Fig. 2, further increased the enzymes' catalytic activity, the storage stability, and the reusability of the hybrids. Hence, more favorable features in the biocatalyst and more significant removal of the dyes tested Bromophenol Blue, Coomassie Blue, and Xylene Cyanol were noticed.

Figure 2 - Laccase hybrid nanoflowers crosslinked with glutaraldehyde
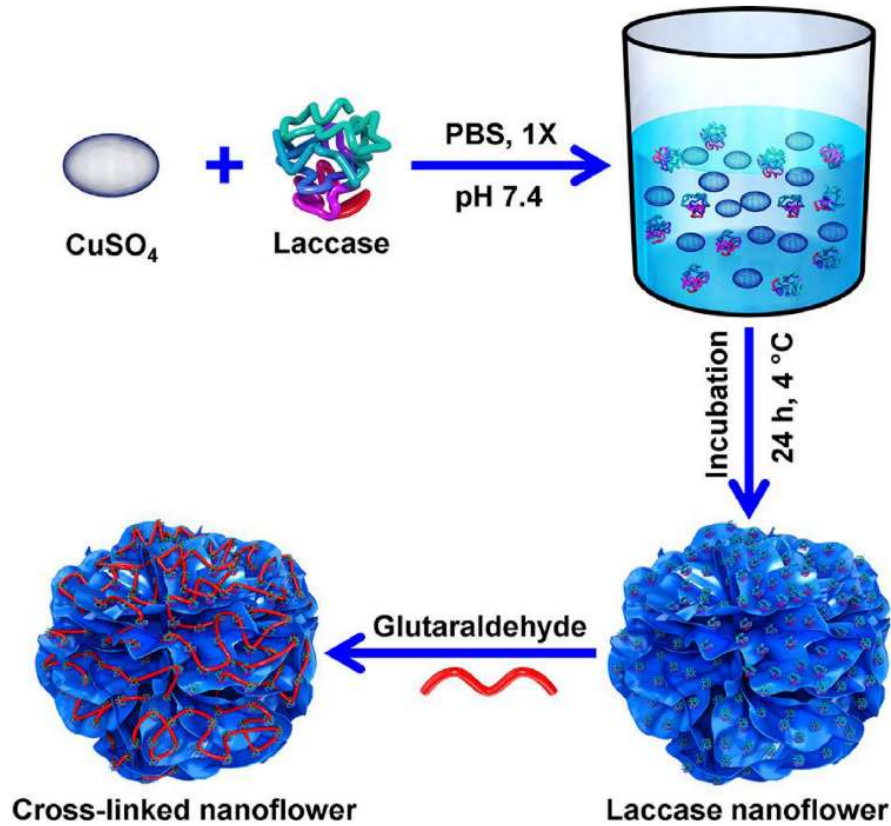
Source: Patel *et al.*, 2018.

Luo *et al.* [88] proposed a supported growth of laccase-copper structures on 3D hierarchically porous nanofibrous poly (vinyl alcohol-co-ethylene) (PVA-co-PE) membrane to improve mechanical features of the hybrid nanoflowers. The scheme of PVA-co-PE nanofibrous membrane synthesis using poly (methyl methacrylate) (PMMA), adsorption of copper ions, and subsequent formation of supported nanoflowers is presented in Fig. 3. The authors showed the hybrids' use for different degradation dyes, such as reactive blue 2, acid blue 25, acid yellow 76, and indigo carmine, with a degradation efficiency of 83.59%, 86.35%, 90.2%, and 99.5%, respectively.

Figure 3 - Hybrid nanoflowers growth onto porous nanofibrous membrane
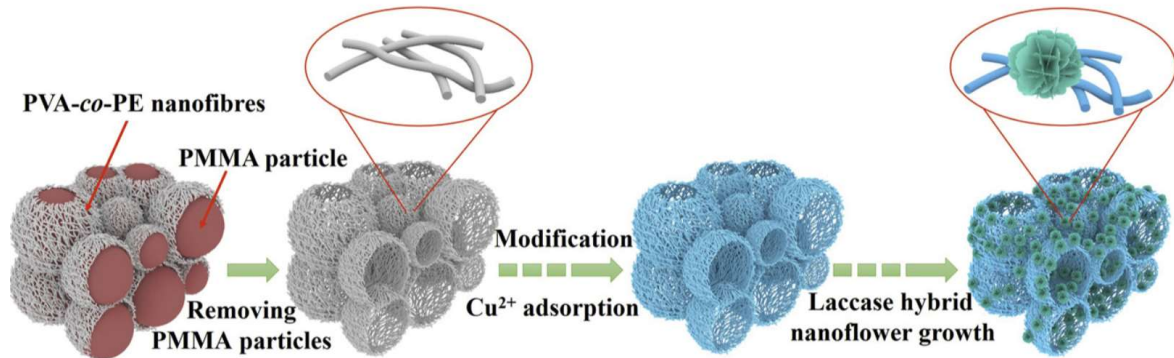
Source: Luo *et al.*, 2020.

Using Turkish black radish peroxidase-Cu^{2+} hybrids, Altinkaynak *et al.* [86] studied the Victoria Blue dye removal from water. The nanoflowers synthesized could be reused up to ten times efficiently, with dye removal decreasing from 90% in the first use to 77% in the tenth.

Egg white and copper ions hybrid nanoflowers developed by Altinkaynak *et al.* [87] were applied to remove direct dyes. Although they do not contain an isolated enzyme in their structure as an organic portion, only the proteins present in egg white, the hybrid structures could act as phenol oxidases and peroxidases. Promising results of up to 80% of color removal from water were observed, proving the possible applicability of this technique using egg white for biocatalytic properties.

Wang *et al.* [15] synthesized hybrid nanoflowers capable of degrading the methyl violet dye using chloroperoxidase with copper, cobalt, and cadmium phosphates. All formed hybrids, each with a metallic phosphate, were able to remove more than 98% of the dye in the solution, proving the high catalytic activity of the structures.

Moreover, Maurya, Nadar et Rathod [14] have shown that not only a free enzyme can be used as the organic portion of hybrid nanoflowers. The authors have proved that a previous mixing of laccase and lysine, a positively charged amino acid, resulted in a higher activity of the free enzyme. Then, this blend of organic components was used with copper ions and sodium phosphate to synthesize efficient hybrid nanoflowers, capable of degrading 89% of a reactive blue 4 dye solution after 1 h.

Different immobilization methods can be used concurrently to improve biocatalyst features, such as increased catalytic activity and ease of separation. Fu, Xiang, and Ge [89] produced magnetic nanoparticles from hybrid copper phosphate and laccase nanoflowers. The biocatalyst reached a degradation of 100% of bisphenol A in the first use and 95% in the fifth use, proving the efficient reusability of the immobilized enzyme.

2.2.2.1 Hydrolysis and digestion of proteins

Lin *et al.* [90] developed hybrid nanoflowers of copper phosphate and trypsin, aiming to degrade two proteins: BSA and HRP. Compared with the free form, the immobilized enzyme showed similar sequence coverage and peptide combination results. However, the results that were obtained in 24 h with the free enzyme were achieved in just 1 min by the nanoflowers, indicating a significant improvement in protein digestion.

Memon *et al.* [82] produced hybrid nanoflowers of alkalase and calcium ions to hydrolyze isolated soy protein, leading to better bioactive properties of these compounds. In addition to demonstrating 90% activity after seven cycles, the immobilized enzyme generated a soy protein hydrolyzate with better solubility than the free enzyme, high radical scavenging capacity, and functional calcium-binding capacity, the potential application of hybrids also in the food industry.

Feng *et al.* [81] have synthesized papain-copper phosphate-magnetic nanoflowers to hydrolyze the cow's milk allergenic proteins. The hybrids had shown an activity 1556% higher compared to free alkaline papain. Furthermore, since the structures were easily separated from the bulk reaction, they could hydrolyze allergic proteins without adding even more free protein to the milk.

2.2.2.2 Hydrolysis of lactose

Organic-inorganic hybrids have their features based on their composition. Talens-Perales *et al.* [93] have synthesized hybrid nanoflowers to hydrolyze lactose with various metal ions – of Cu^{2+}, Mn^{2+}, Zn^{2+}, $Co^{2+,}$ and Ca^{2+} – as the inorganic component and β-galactosidase from *Thermotoga maritima*, a thermophilic bacterium, as the organic part. Besides the already expected differences in the nanoflowers morphologies using different ions, the authors have shown that enzyme activities also depend on the metal used. While structures with Mn^{2+}, $Co^{2+,}$ and Ca^{2+} showed similar activity to the same amount of free enzyme, Zn^{2+} and Cu^{2+} presented activity decreases of 2 and 10-fold, respectively. Although copper ions are commonly used in hNFs synthesis, they are known inhibitors of the lactase employed in the assays. By testing the nanoflowers' activity, stability, and recycling, Talens-Perales *et al.* have proved that calcium-containing structures showed better features than the hybrids with other tested metal ions in this case.

2.2.3 Biosensors production

2.2.3.1 Phenol and hydrogen peroxide detection

The use of nanoflowers in biosensors' production to detect compounds has been studied since the first applications of this technique. In this sense, compounds of environmental interest such as hydrogen peroxide and phenol, highly toxic, are examples of research objects to be detected and quantified. Zhu *et al.* [35] reported to have developed a fast and easy method of detecting phenol using nanoflowers, represented in Fig. 4. The organic-inorganic hybrids, synthesized using copper ions and laccase, were immobilized in a syringe filter (pore diameter of 0.2 µm). When passed through the filter containing the laccase, phenol solutions in concentrations of 0.4 to 50 µg.mL^{-1}, in the presence of 4-aminoantipyrine (4-AAP), formed a pink chromophore group. The formation of this chromophore allowed the quantification of phenol in the samples. Activity assays carried out by the authors demonstrate an activity of nanoflowers equivalent to about 200% of the free enzyme for the oxidation of phenol [35].

Figure 4 – Phenol biosensing with laccase nanoflowers
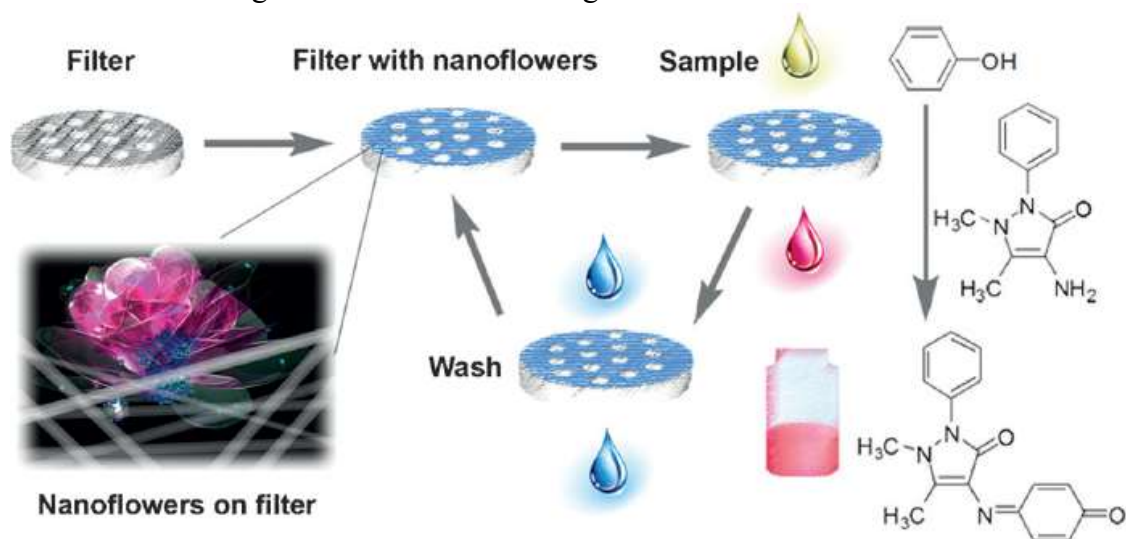
Source: Zhu *et al.*, 2013.

Based on the oxidation of compounds and the presence of a chromophore group, it was observed the use of different enzymes as catalysts for the same reaction was employed by Zhu *et al.* [35]. For example, Lin *et al.* [42] synthesized hybrids of copper phosphate and HRP to detect phenol and hydrogen peroxide. The authors found an increase of 506% in the activity of the nanoflowers compared to the free HRP enzyme in the solution [42]. Also, to detect hydrogen

peroxide, Zhang *et al.* [24] produced organic-inorganic hybrids from catalase and copper phosphate with the aid of a sonicator bath. The use of this technique allowed the structures to be wholly formed in 30 min. The synthesized nanoflowers showed, in addition to the increased activity, a significant gain in their stability. After 28 days, catalase lost 62% of its initial activity in its free form, while catalase nanoflowers continued with 90% of their initial activity [24].

2.2.3.2 Glucose detection

Multifunctional biocatalysts, obtained by immobilizing multiple enzymes simultaneously, have broad applicability in "cascade" reaction systems, a complex system in which the product, or by-product, of a reaction acts as a substrate for the subsequent reaction [106]. This concept was explored by Sun *et al.* [94] when producing hybrid GOx and HRP nanoflowers with copper phosphate, aiming to develop a glucose biosensor.

The synthesis of these nanostructures allowed the combination of a cascade reaction, schematized in Fig. 5, catalyzed by two enzymes. The first reaction of glucose transformation by GOx has as a by-product hydrogen peroxide, which is catalyzed by HRP forming a chromophore group, allowing the detection and quantification of the initial glucose [94].

Figure 5 – Glucose detection mechanism by Gox-HRP hybrid nanoflowers
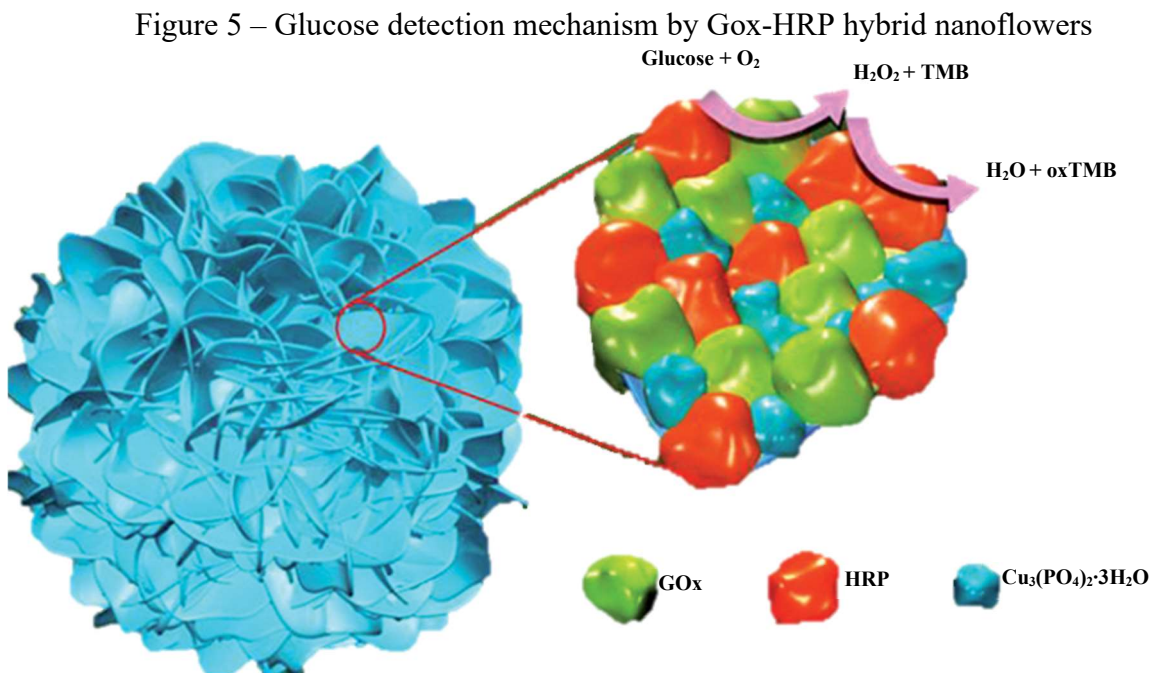
Source: Sun *et al.*, 2014.

Ariza-Avidad, Salinas-Castillo, and Capitán-Vallvey [85] used nanoflowers with the same composition to produce a three-dimensional microfluidic device on paper, aiming at the colorimetric detection of glucose. The biosensor, which reached detection limits of 15.6 $\mu mol.L^{-1}$, demonstrated easy reuse and high stability of the micro-reactor for up to 75 days [95].

Similar detection ranges were obtained by hybrid nanoflowers of GOx and copper ions synthesized by Batule *et al.* [23]. According to the authors, the biocatalyst effectively detected glucose up to 3.5 $\mu mol.L^{-1}$, demonstrating practical applicability since the concentration of this molecule in human blood is in the order of some $mmol.L^{-1}$ [23].

Not only different organic compounds can be used in the same nanoflowers to enhance their features. Cheon *et al.* [22] have obtained prosperous structures by incorporating GOx-copper phosphate hybrid nanoflowers into Fe_3O_4 magnetic nanoparticles (MNPs). First, these MNPs, previously reported to have peroxidase-like activity [107], were amine-functionalized. Then, it was possible the electrostatic attraction of GOx and the amino groups in the MNPs. Finally, in the presence of phosphate and copper groups, the nanoflower's formation and growth occurred. By using a cascade reaction, catalyzed first by the GOx and then by the MNPs peroxidase-like activity, the authors have successfully reused the glucose biosensor up to ten times, with 90% of the initial activity remaining. A scheme of the biosensor produced by the authors is shown in Fig. 6, representing the conversion of Amplex UltraRed (AUR) into a fluorescent product.

Figure 6 – Glucose biosensing by the action of MNPs-Gox NFs

Source : Cheon *et al.*, 2019.
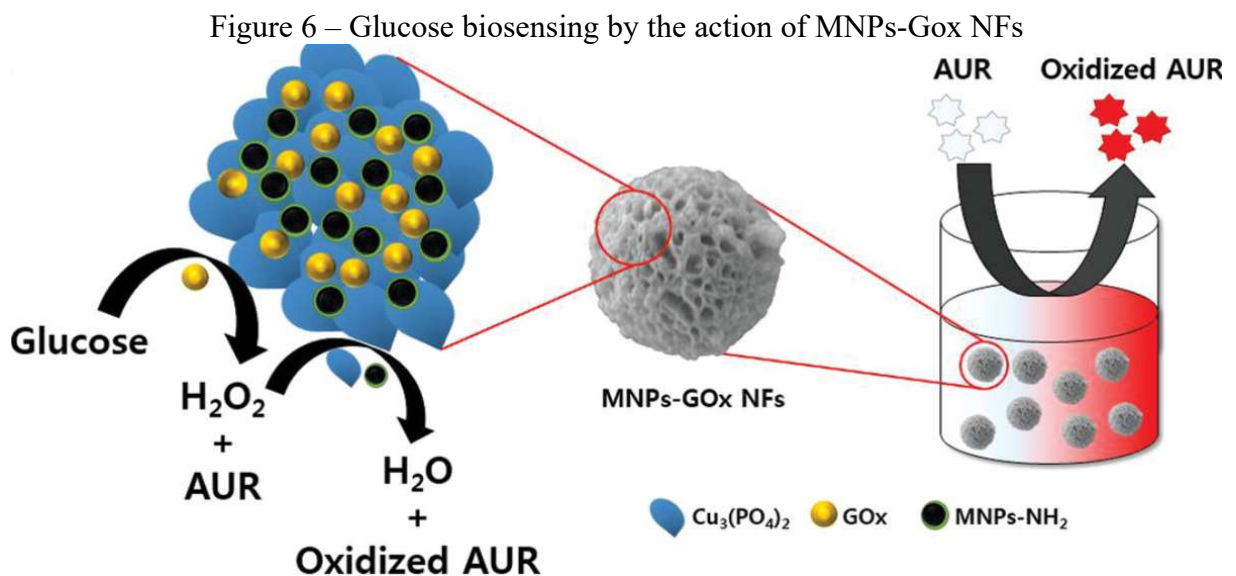
Li *et al.* [21] performed the *in situ* synthesis of nanoflowers directly on cellulose paper to optimize the manufacture of a glucose biosensor. Initially, manganese sulfate, the donor of the metallic ions of the hybrids, was added on paper, followed by a phosphate solution containing GOx. The biosensor showed high specificity for detecting glucose in complex samples, demonstrating high applicability for *on-site* analyses.

2.2.3.3 Pathogens detection

The early detection of pathogens present in food and water can mean more safety and a considerable decrease in spending on disease treatment [108]. Biosensors of various performances and forms have been developed to make their applications even simpler and more precise [109]. The use of hybrid nanoflowers proves to be a viable path with great potential within biosensors development.

A biosensor based on hybrid nanostructures of concanavalin A, GOx, and calcium ions for *E. coli* O157: H7 detection was developed by Ye *et al.* [26]. The biosensor, illustrated in Fig. 7, was developed based on the affinity of concanavalin A and the lipopolysaccharides O-antigen, present in the structure of the bacteria, and the GOx ability to convert glucose into gluconic acid. As gluconic acid increases the medium's acidity under analysis, the bacteria could be quantified by analyzing the pH.

Figure 7 – E. coli detection through pH changes by nanoflowers catalysis
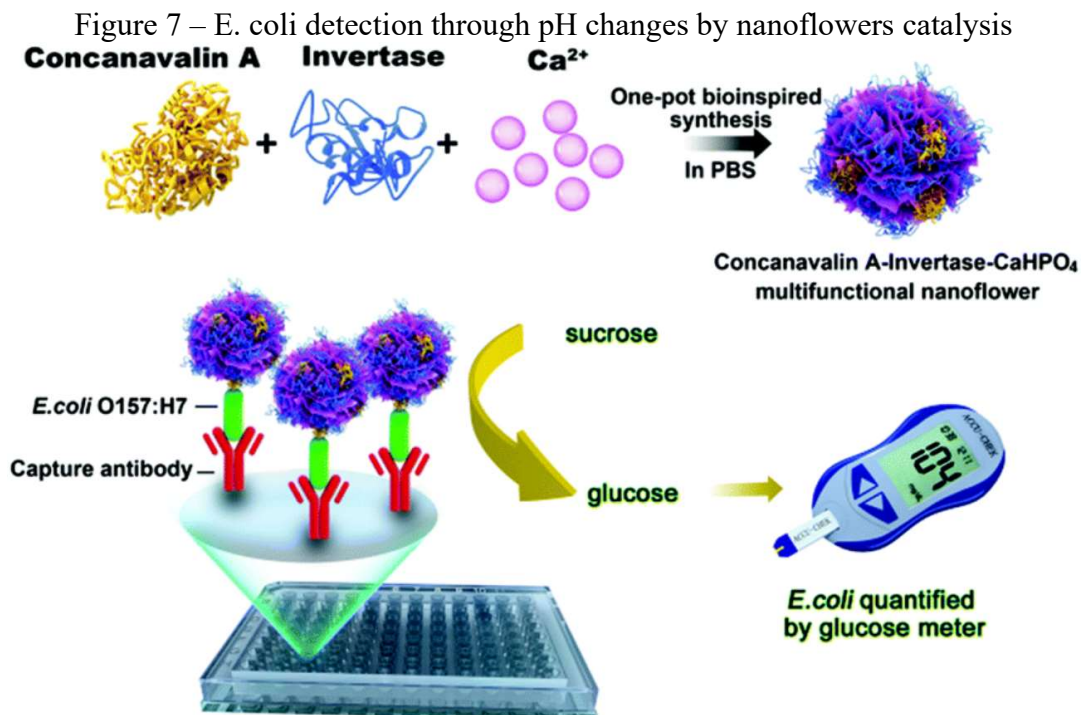
Source : Ye *et al.*, 2016.

Wang *et al.* [87] produced hybrid nanoflowers of hemin and concanavalin A with copper phosphate to detect the same bacteria, which showed a peroxidase-like activity. Using a colorimetric biosensor developed based on the performance of the described nanoflowers and in the presence of diammonium salt, adequate detection of the microorganisms was observed up to the estimated limit of 4.1 CFU.mL^{-1}.

It is also known that different bacteria can be responsible for infections in the urinary tract, and the treatment is more appropriate when the responsible microorganism is identified correctly [110]. Thus, Li *et al.* [98] developed an electrochemical biosensor capable of identifying and quantifying bacteria present in the urine through the action of hybrid nanoflowers of GOx, HRP, and copper ions. This sensor was based on recognizing specific T4 phages combined with an electrical signal amplification resulting from reactions catalyzed by nanoflowers. The authors reported an excellent detection limit of 1 CFU.mL^{-1} using this technique.

2.2.3.4 Epinephrine detection

Epinephrine or adrenaline, considered both a hormone and a neurotransmitter, can treat anaphylactic shock, bronchial asthma, and heart disease, and abnormal variations in body levels can be a symptom of diseases such as Parkinson's [111]. Colorimetric biosensors from nanoflowers show fast and straightforward alternatives for detecting this compound in solution.

Batule *et al.* [78] produced hybrid nanoflowers of laccase and copper phosphate via sonication to detect adrenaline. A visual comparison of the use of the free enzyme and nanoflowers showed a much more accentuated color in the detection of adrenaline through immobilized structures, confirming the higher activity.

Using lactoperoxidase as the enzyme, Altinkaynak *et al.* [25] proved the employment of the immobilized biocatalyst in the visual detection of both adrenaline and dopamine. The activity of nanoflowers increased up to 630% for dopamine detection and up to 570% in the detection of adrenaline compared to equivalent amounts of the free lactoperoxidase.

2.2.3.5 Organophosphorus pesticide detection

Despite being controlled due to their harmful health effects, organophosphorus pesticides have frequent use in modern agriculture. For this reason, the detection of its residues might be an important tool for the environmental safety [112,113].

In view of this, Jin *et al.* [96] developed an electrochemical and colorimetric biosensor based on hybrid nanoflowers of acetylcholinesterase and choline oxidase with copper ions. Using cascade reactions catalyzed by the enzymes present in the nanostructures, the authors achieved excellent detection levels of 6 phentograms per milliliter or 6×10^{-15} g.mL^{-1}.

2.3 PERSPECTIVES

Even though hybrid nanoflowers tend to show several advantages compared to traditional immobilization techniques, their applications also might present some challenges. Among those are the difficulty of separation and consequent reuse, considering the small size of the hybrid structures; the commonly long incubation time of 3 days; the structures' mechanical stability; and the low productivity of hybrids in each batch [17,85,89,91].

Against this background, some actions are made to assure better features to the structures. For example, some changes in synthesis' conditions, or the concomitant use of different techniques, such as crosslinking or the production of magnetic nanoparticles.

Despite all those modifications, and considering their characteristics, the organic-inorganic hybrid nanoflowers have in biosensors production a great potential application. Enzymatic biosensors can be produced with an enormous variety of biocatalysts, and they usually do not need a great amount of enzyme to be produced. Furthermore, hybrid nanoflowers can be synthesized directly onto the biosensor, what could facilitate its reuse and could also reduce the production costs.

2.4 PHENOL AS AN ENVIRONMENTAL POLLUTANT

Phenol, a colorless-to-white solid with a melting point of about 40.9 ºC and a molecular formula of C_6H_5OH, is both a natural and a synthetic chemical. Phenolic compounds also represent a class of organic chemicals, all of them being derivatives of phenol. Common phenolic compounds and their respective applications are presented in Table 2.

Table 2 - Phenolic compounds: structures and applications

(to be continued)
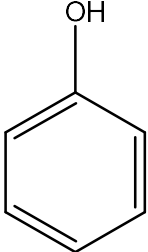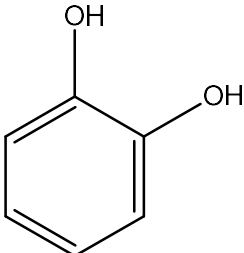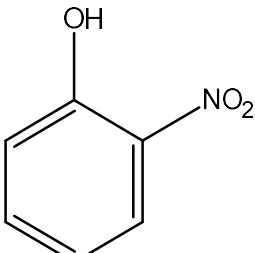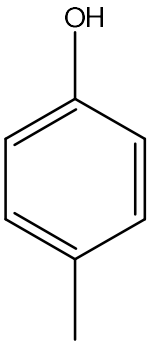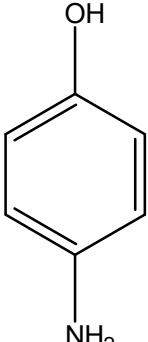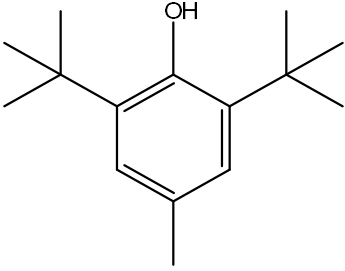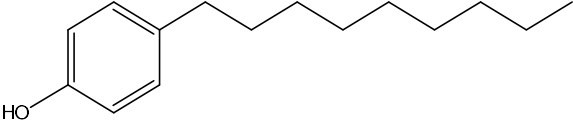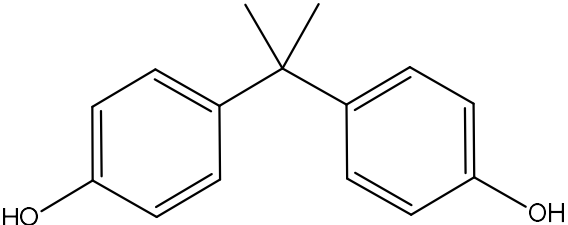
Compound	Structure	Applications
Phenol		Chemical industry (e.g., resins, plastics, pesticides, dyes), coal processing, metallurgic, etc.
Catechol		Photography, rubber, dyes, insecticides, cosmetics, etc.
2-nitrophenol		Polymers, drugs, photography, etc.
4-methylphenol		Insecticides, cosmetics, explosives, etc.
4-aminophenol		Oils, lubricants, photography, etc.

Table 2 - Phenolic compounds: structures and applications

(conclusion)

Compound	Structure	Applications
Buthylohydroxy-toluene		Gasoline, lubricants, oils, waxes, rubber, plastics, etc.
4-nonylphenol		Emulsifiers, wetting agents, dispersing agents, etc.
Bisphenol A		Lubricants, epoxy-resins, rubber, plastics, etc.

Source: adapted from Michalowicz and Duda (2007)[114]

To determine the environmental fate of organic pollutants, such as phenolic compounds, however, might be a challenge given the complexity of measuring their actual concentration all over the world. From this perspective, models for environmental fate have been extensively developed to predict the spread of chemicals through the environment [115]. The theoretical distribution of phenol in the environment estimated by Mackay's model (level 1) is presented in Table 3.

Table 3 - Theoretical phenol distribution in the environment

Environment phase	Percentage
Air	0.8
Water	98.8
Soil	0.2
Sediment	0.2

Source: adapted from European Union Risk Assessment Report: phenol [116]

Accordingly, water bodies represent the main target of phenols in the environment. Aqueous phenol in nature might portray a persistent pollutant, with toxic effects, including cancerogenic, from chronic or acute exposure in humans and animals [117,118]. For this reason,

phenolic compounds are considered pollutants of priority concern by the European Union (UE) and by the United States Environmental Protection Agency (USEPA) [116,119].

Phenols in the environment have different sources. One is represented by the naturally occurring phenols found in several living beings, from fungus to plants and animals. Another natural origin of phenol is throughout plants and animals' decomposition [118]. However, many phenols in water bodies come from manufactured chemicals in industrial, agricultural, and domestic wastes. Phenol is generally used as an intermediate in chemical synthesis. Among those are synthesizing other chemicals (bisphenol A, salicylic acid, and alkyl phenols, for example), phenolic resins, paints, plastics, disinfectants, pesticides, cosmetics, and medical preparations [116,118]. Paper and cellulose, petroleum refining, pharmaceutical, and metal coating industries are also great consumers and producers of phenolic compounds [27,28]. The inappropriate discharge of effluents from those industries might lead to environmental contamination in water bodies.

Phenol toxicity in humans is observed on multiple scales. Phenol's acute effects include skin, eyes, and mucous membranes, inhalation, and dermal contact. Irregular breathing, muscle weakness, tremors, convulsions, coma, and respiratory arrest at lethal doses are also possible [119]. Phenol's chronic effects might include anorexia, weight loss, diarrhea, vertigo, gastrointestinal irritation, muscle pain, dermal inflammation, necrosis, arrhythmias, and blood, liver, kidney, respiratory and cardiovascular effects [119].

Nevertheless, not only humans can be affected by phenol toxicity. The entire aquatic ecosystem might be affected by phenolic compounds in water, from accidental leakages, natural or anthropogenic sources [114,118].

Effective detection of phenol in water bodies is essential to a rapid action and to minimize possible environmental damage when it is in high concentrations. Against it, many strategies have been researched, with a special focus on biosensors with laccase, tyrosinase, and peroxidase enzymes, to detect phenol in solution [29–46].

3 MATERIAL AND METHODS

3.1 CHEMICALS AND MATERIALS

Horseradish peroxidase (HRP) was obtained from Toyobo (Brazil). 4-AAP, H_2O_2 (35%), Na_2HPO_4, NaH_2PO_4, NaCl, $CaCl_2$, and $CuSO_4$ of analytical grade were employed in the assays. PVDF Hydrophilic Membrane (GVS, USA) with a pore diameter of 0.22 μm was used to produce the biosensors. Distilled water was used in all experiments.

3.2 PREPARATION OF COPPER-HRP AND CALCIUM-HRP HYBRID NANOFLOWERS

The copper-HRP hybrid nanoflowers (Cu^{2+}-hNF) were synthesized following previously reported methods [13,42,93,120–122] with some modifications. In a typical experiment, 67 μL of $CuSO_4$ (120 mM) were added to 10 mL of phosphate-buffered saline (PBS) (100 mM, pH 7.4) with 0.1% NaCl (w/w) containing HRP in different concentrations from 0.1 to 1.0 mg.mL^{-1}. This mixture was stirred with a vortex for 30 s and then incubated at 4 °C for 72 h. The precipitated with the hybrids was collected through centrifugation at 4000 rpm for 15 min. Calcium-HRP hybrid nanoflowers (Ca^{2+}-hNF) were synthesized with the same procedure, using the best enzyme concentration from Cu^{2+}-hNF experiments and 67 μL of $CaCl_2$ (120 mM) as the donor of calcium ions.

3.3 CHARACTERIZATION OF COPPER-HRP AND CALCIUM-HRP HYBRID NANOFLOWERS

The morphology of Cu^{2+}-hNF and Ca^{2+}-hNF was analyzed by scanning electron microscopy (SEM, JEOL JSM-6390LV). The electron microscope was equipped with energy-dispersive X-ray spectroscopy (EDS) to determine the elemental composition of the structures as well. Samples were prepared by dripping 10 μL of the hNFs suspension onto polyvinylidene fluoride (PVDF) membranes with 0.22 μm of pore size, which were dried in a desiccator at room temperature for 24 h. Functional groups present in the hybrids and the free enzyme were identified and characterized by Fourier transform infrared spectroscopy (FTIR, AGILENT TECHNOLOGIES – Cary 660) from 400 to 4000 cm^{-1}. Powdered X-ray diffraction (XRD, Enraf – Nonius, model Cade – 4) technique within the 2θ range from 5° to 60° was used to identify the crystal structure of HRP hybrid nanoflowers.

3.4 ENZYME ACTIVITY ASSAYS

The peroxidase activity was determined using a method previously proposed by Trinder (1969) with modifications. This approach, which employs 4-AAP as hydrogen donor, is measured spectrophotometrically by the hydrogen peroxide degradation and consequent formation of quinoneimine, a pinkish antipyrine dye [123,124]. This reaction is represented in Fig. 8:

Figure 8 - Scheme of the peroxidase-catalyzed reaction of H_2O_2, phenol, and 4-AAP
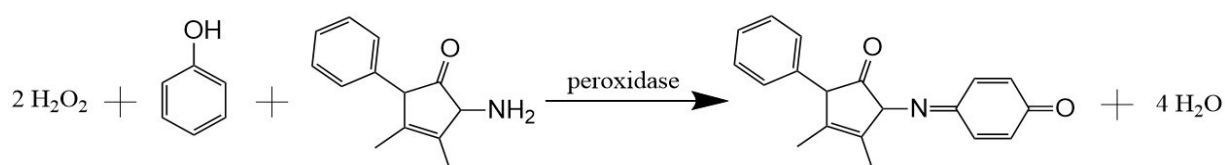
For the assay at 25 °C, 1.5 mL of 0.0017 M hydrogen peroxide (in PBS 0.2 M, pH 7.4) was mixed with 1.4 mL of a solution containing 0.0025 M 4-AAP and 0.17 M phenol. The reaction was started by adding 0.1 mL of free HRP 0.25 mg.mL^{-1}, Cu^{2+}-hNF 1.0 mg.mL^{-1} or Ca^{2+}-hNF 0.5 mg.mL^{-1} suspension to the reaction medium. The absorbance was measured after 1 min in 510 nm by spectrophotometry (Hitachi, model U–2900). Different enzyme concentrations were used so the absorbance variance after 1 min was within the detection limit of the spectrophotometer in all cases. In this work, one HRP activity unit (U) was defined as the amount of enzyme that produces 1 mmol of quinoneimine per minute under experimental conditions. Enzymatic activity of free enzyme and hNFs were calculated with the Eq. 1 [124]:

$$A = \frac{\Delta Abs_{510}}{\varepsilon \times b \times t} \qquad \text{Eq. 1}$$

Where A is the enzymatic activity of HRP (U.L^{-1}), ΔAbs_{510} is the absorbance variance at 510 nm, ε is the molar absorption coefficient of quinoneimine dye (6.58 L.mmol^{-1}.cm^{-1}), b is the light path length (1 cm), and t is the reaction time (1 min).

3.5 ENCAPSULATION YIELD

The encapsulation yield (Y) is used to determine the percentage of the initial free enzyme reduced to the immobilized form. The enzymatic activities of the free HRP and the hybrid nanoflowers were carried as described previously in section 3.4. Subsequently, the immobilization yield was calculated using Eq. 2:

$$Y\ (\%) = 100 \times \left(\frac{A_i - A_s}{A_i} \right) \qquad \text{Eq. 2}$$

Where A_i is the initial activity in the HRP solution and A_s is the activity of the supernatant obtained by centrifugation of the reaction medium after the hybrid nanoflowers synthesis.

3.6 PH AND TEMPERATURE EFFECT ON THE ENZYME ACTIVITY OF THE FREE HRP AND HNF PREPARATIONS

Different buffers, such as McIlvaine buffer 0.1 M for pH 3.0, 4.0 and 5.0; phosphate buffer 0.1 M for pH 6.0, 7.0 and 7.4; Tris–HCl buffer 0.1 M for pH 8.0 and 9.0; Sorensen's glycine buffer for pH 10.0, 11.0 and 12.0; and NaOH 0.1 M for pH 13.0 were used to produce 0.0017 M hydrogen peroxide solution to evaluate pH influence on the enzyme activity. The activity assays were carried out using the phenol and 4-AAP method previously described.

The reagents and enzymatic preparations were incubated for 5 minutes in a thermostatic bath (SolidSteel, Model SSDc – 10 L) in several temperatures (from 25 to 70 °C) before the reaction start. The whole reaction was carried as above stated, within pH 7.4 buffer, in the intended temperature. Both pH and temperature-dependent activities were expressed as relative activities (%), where the higher value for each sample was set as 100%. Error bars represent the standard deviation of three independent experiments.

3.7 EFFECT OF THE PH AND TEMPERATURE ON STABILITY OF THE FREE HRP AND HNF PREPARATIONS

To assess the pH influence on the stability of free and immobilized preparations, all hNFs produced in a typical synthesis, as well as the equivalent amount of HRP, were suspended in 2.0 mL of various buffer solutions: citrate buffer 0.1 M for pH 4.0 and 5.0; phosphate buffer for pH 6.0 and 7.4; Tris-HCl buffer 0.1 M for pH 8.0 and 9.0. The activities were measured

using 0.1 mL of the enzyme or hNFs preparations in the intended pH, following the identical procedure described in section 3.4 at different times, from 0 to 8 h.

The thermal stability of the free enzyme and hNFs was appraised in the following way: first, all hNFs synthesized in a typical experiment were suspended in 2.0 mL of PBS 0.1 M, pH 7.4. A solution of an equivalent amount of the free enzyme was made the same way. Then, these preparations were placed in a thermostatic bath at settled temperatures of 50, 60, and 70 ºC. Finally, 0.1 mL was taken from each sample at different times (0, 2, 4, 6, and 8 h), and activity was measured at room temperature, following the phenol method previously described. The stability was estimated by plotting the relative activity (%) as a function of the time the enzyme was exposed to each condition, considering the initial activity value for each sample as 100%.

3.8 DETERMINATION OF KINETIC PARAMETERS K_M, V_{MAX}, AND K_{CAT}

Initial specific reaction rates (V_0) were obtained by measuring the absorbance variation at 25 °C, 510 nm, and 1 min of reaction time. The reaction medium was prepared mixing 0.1 mL of enzyme sample (HRP 0.25 mg.mL^{-1}, Cu^{2+}-hNF 1.0 mg.mL^{-1} or Ca^{2+}-hNF 0.5 mg.mL^{-1}), 1.5 mL of 0.0017 M hydrogen peroxide in PBS 0.2 M and pH 7.4, 0.7 mL of 0.005 M 4-AAP and 0.7 mL of phenol in different concentrations, from 3 to 400 mM. V_0 values were calculated with Eq. 3:

$$V_0 = \frac{\Delta Abs_{510}}{\varepsilon \times b \times t \times C_E} \qquad \text{Eq. 3}$$

Where V_0 is the initial specific reaction rate (µmol.min^{-1}.mg^{-1}), ΔAbs_{510} is the absorbance variance at 510 nm, ε is the molar absorption coefficient of quinoneimine dye (6.58 L.mmol^{-1}.cm^{-1}), b is the light path length (1 cm), t is the reaction time (1 min), and C_E is the enzyme concentration in the assay (mg.mL^{-1}). Results are presented as average result ± standard deviation, which was estimated from the Lineweaver-Burk graph, plotted in Sigmaplot 14.0, using GNU Octave 6.2.0 software.

Kinetic parameters K_M (µmol.mL^{-1}) and V_{max} (µmol.min^{-1}.mg^{-1}) of Michaelis-Menten model for simple enzymatic reactions (Eq. 4) were then determined for the free enzyme and both hybrids, using phenol as the substrate.

$$V_0 = \frac{V_{max}[S]}{K_M + [S]} \qquad\qquad \text{Eq. 4}$$

Where V_0 is the initial specific reaction rate ($\mu mol.min^{-1}.mg^{-1}$), V_{max} is the maximum specific reaction rate ($\mu mol.min^{-1}.mg^{-1}$), K_M is the Michaelis constant ($\mu mol.mL^{-1}$), and [S] is the substrate concentration ($\mu mol.mL^{-1}$).

Subsequently, the turnover number, or k_{cat}, was also determined. Values were obtained by using Eq. 5:

$$k_{cat} = V_{max}M_{HRP} \qquad\qquad \text{Eq. 5}$$

Where k_{cat} is the turnover number (min^{-1}), V_{max} is the maximum specific reaction rate ($\mu mol.min^{-1}.mg^{-1}$), and M_{HRP} is the molar weight of the HRP enzyme (44.0 $mg.\mu mol^{-1}$).

3.9 MEMBRANE-BASED PHENOL DETECTION USING COPPER-HRP AND CALCIUM-HRP HYBRID NANOFLOWERS

A qualitative membrane-based biosensor was developed by employing a craft-cutting technique to provide a cost-efficient phenol detector. First, 1 cm² square was cut from a PVDF membrane, with 0.22 μm of pore size, and 10 μL of Cu^{2+}-hNF or Ca^{2+}-hNF 1.0 $mg.mL^{-1}$ suspensions were dripped onto the squares and left to dry in a desiccator at room temperature for 12 h. For comparing purposes, control biosensors were made with 10 μL of an equivalent amount of the free enzyme. Subsequently, the efficacy of the biosensors for phenol detection was investigated with 50 μL of a sample solution. This solution, which contained H_2O_2 0.88 $\mu mol.mL^{-1}$, 4-AAP 1.1 $\mu mol.mL^{-1}$ and phenol in different concentrations from 0.72 to 24.00 $\mu mol.mL^{-1}$ in PBS 0.2 M with pH 7.4, was dripped onto the biosensors. As a result, a pink color appears on the hNFs membranes to prove the presence of phenol.

4 RESULTS AND DISCUSSION

4.1 SYNTHESIS AND CHARACTERIZATION OF CU^{2+}-HNF AND CA^{2+}-HNF

As a recent and promising enzyme immobilization technique, organic-inorganic hybrid nanoflowers are micro-sized structures that present nanoscale patterns and tend to exhibit flower-like shapes [122]. The growth mechanism of these nanoflowers has been widely described [13,42,92,94,125]. Briefly, three steps can summarize the mechanism: nucleation, growth, and compilation [120,126]. First, amide groups present in the enzyme backbone complex with metal ions, while the same ions react with $(PO_4)^{3-}$ from PBS to form primary crystals of $Cu_3(PO_4)_2 \cdot 3H_2O$ or $CaHPO_4$ and $Ca_3(PO_4)_2 \cdot 2H_2O$ embedded with HRP. These complexes act as nucleation points for hybrid nanoflowers assembly; therefore, they depend on the enzyme in the synthesis medium. It has been shown that lower enzyme concentrations lead to fewer nucleation points and consequently hybrids with greater diameter [77,127]. The growth stage, which occurs anisotropically, is marked by the continuous addition of enzyme molecules to those primary crystals, creating the first hybrid petals. Then, the compilation stage is observed, where the enzyme induces the metal-phosphate crystallization into a basis for new petals and simultaneously attaches petals in flower-like structures [120].

4.1.1 Scanning electron microscopy

The effect of the initial concentration of HRP in the morphology of Cu^{2+}-hNF was investigated by SEM analysis (Fig. 9). With 0.10 $mg_{HRP}.mL^{-1}$, hybrid structures (Fig. 9A) showed loose petals, although they had adequate size and formation. Higher concentrations of 0.25, 0.50, and 1.00 $mg_{HRP}.mL^{-1}$ had led to tightened petals and consequent grater ratio surface area per volume (Fig. 9B, 9C, and 9D). It is noticeable that Cu^{2+}-hNF produced with 0.25 $mg_{HRP}.mL^{-1}$ exhibited greater spherical shape consistency and distinct petal-like structures.

Figure 9 - SEM images of Cu^{2+}-hNF produced with different initial HRP concentration of (A) 0.10 mg.mL^{-1}, (B) 0.25 mg.mL^{-1}, (C) 0.50 mg.mL^{-1} and (D) 1.00 mg.mL^{-1}, at 4 ºC for 72 h
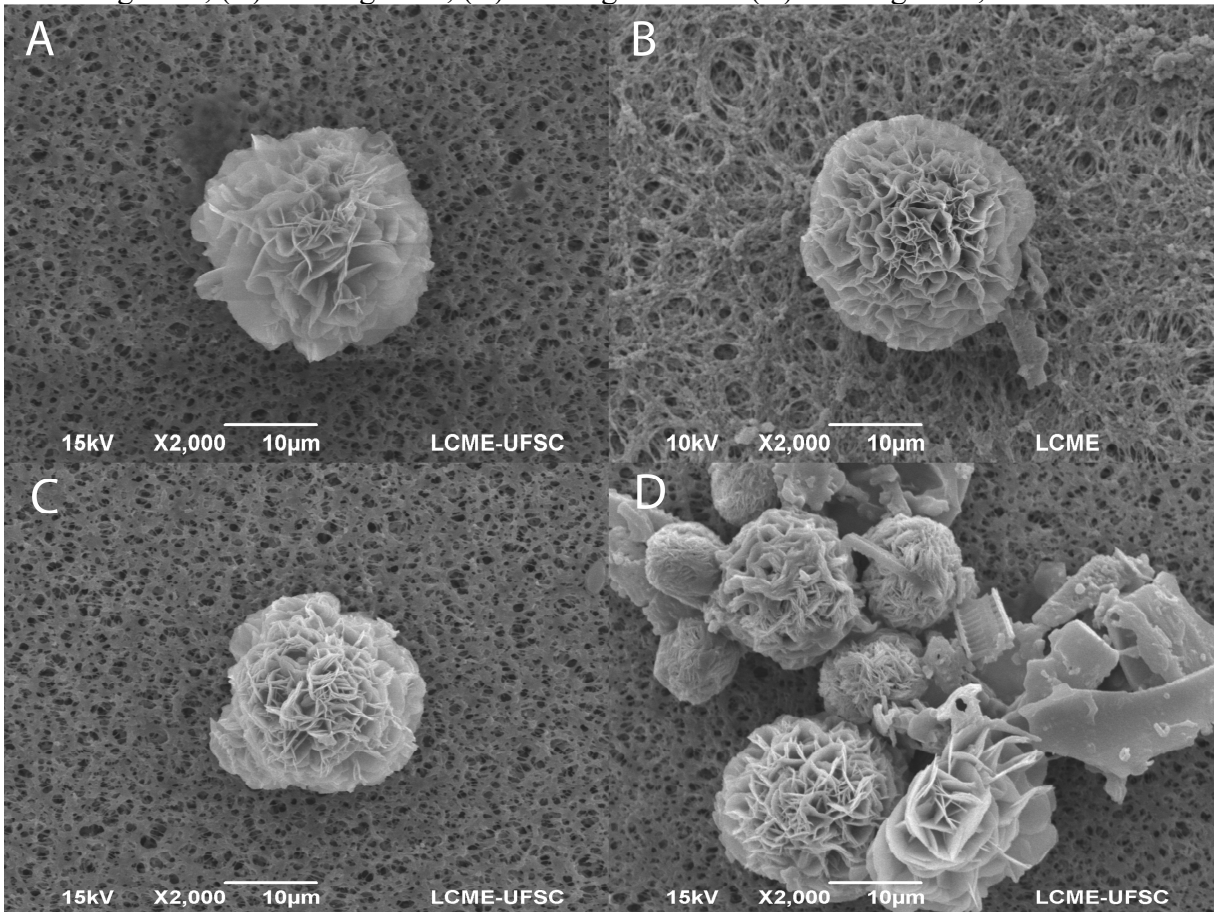
Ca^{2+}-hNF was synthesized using the initial HRP concentration of 0.25 mg$_{HRP}$.mL^{-1} and the same ion concentration of 80 mM, according to good structure formation seen in SEM results of Cu^{2+}-hNF. SEM images of these new hybrids are shown in Fig. 10.

Nevertheless, the flower-like structure was not well determined in this case. The difference between calcium and copper hybrid produced at the same conditions might be explained by the formation of contrasting metal-phosphates structures, mainly amorphous for calcium and crystalline for copper [128]. Ke *et al.* (2016) have shown in their study with lipase-calcium hybrids that the flower-like structure only appeared with the specific PBS concentration of 20 mM. At lower concentrations, there was no complete formation of the petals. In comparison, an excess of calcium phosphate was added to these petals at higher concentrations, and nanoflowers were not seen in either case [76]. Zhang *et al.* (2020) have proved that the calcium ion concentration also influences the hybrid's morphologies. Their work about lipase-inorganic nanoflowers reported that flower-like structures were only observed when calcium ion concentrations higher than 200 mM were used. Below this point, irregular nanoparticles

were formed [19]. Furthermore, Yu and co-workers (2018) have also communicated that calcium-organic hybrids did not present the same evident shape that copper nanoflowers usually do with neither of the six enzymes tested, even though each of them had a distinct appearance [128].

Figure 10 - SEM images of Ca^{2+}-hNF produced with an initial concentration of HRP of 0.25 mg.mL^{-1}, at 4 °C for 72 h
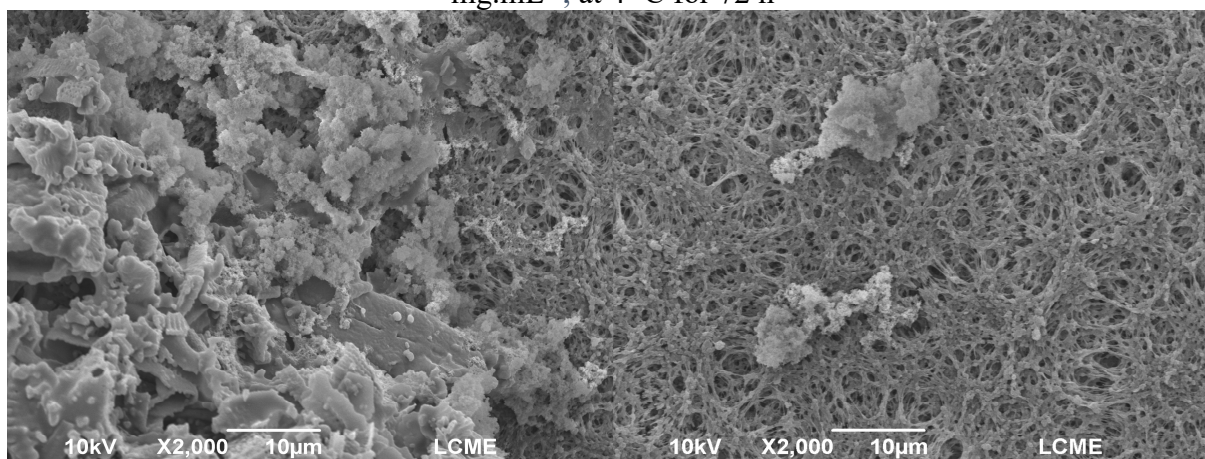
4.1.2 Encapsulation yield

Sheldon and van Pelt (2013) described that the immobilization yield can be precisely established by measuring the residual activity in the enzyme solution after the immobilization process and comparing this value to the initial activity [12]. Different initial enzyme concentrations were tested in hNFs synthesis. The average results of encapsulation yield and respective experimental standard deviations of three independent experiments are shown in Table 4. These results suggest an optimal initial enzyme concentration of 0.25 mg.mL^{-1} for both metal ions used, which leads to a higher encapsulation yield. The higher encapsulation yields were 92.3% and 92.0% for Cu^{2+}-hNF and Ca^{2+}-hNF, respectively. With an enzyme concentration of 0.10 mg.mL^{-1}, this encapsulation yield decreased to 85.7% in Cu^{2+}-hNF and 83.5% in Ca^{2+}-hNF. Likewise, this value was also reduced with an initial HRP of 0.50 mg.mL^{-1} to 89.2% in Cu^{2+}-hNF and 89.4% in Ca^{2+}-hNF. According to this outcome and those published in prior works [22,78,79,81,121], it is possible to deduce that there is an optimal protein concentration that leads to the highest encapsulation yield value. Based on morphologies features observed in Cu^{2+}-hNF and on protein embedding efficiency for both

hybrids, the initial protein concentration of 0.25 $mg.mL^{-1}$ was fixed for all subsequent characterization and application.

Table 4 - Encapsulation yield of HRP based on residual enzyme activity in the supernatant

Metal	Initial enzyme concentration ($mg.mL^{-1}$)	Encapsulation yield (%)
	0.10	85.7 ± 0.7
Cu^{2+}	0.25	92.3 ± 0.2
	0.50	89.2 ± 1.1
	0.10	83.5 ± 0.6
Ca^{2+}	0.25	92.0 ± 0.7
	0.50	89.4 ± 0.3

4.1.3 Energy dispersive X-ray spectroscopy

The EDS technique revealed the elemental composition of hybrid nanoflowers. The EDS spectrum results in atom percentage are found in Table 5. Characteristic peaks of classical elements as C, O, and P commonly reported were observed in both hybrids [19,121,129,130]. Copper was verified in an atom amount of 16.30 % in Cu^{2+}-hNF, while the atom concentration of calcium in Ca^{2+}-hNF was 27.97%, proving the formation of organic-inorganic structures. Chlorine was also recognized in EDS analysis for both hybrids, but more expressively in copper ones. These ions, obtained by NaCl in solution, perform an essential role in hNFs formation [94,95,125]. This was first described by Sun *et al.* (2014) when the authors noted that no nanoflowers were formed without chloride ions [94]. The statement was supported by Somtkurk *et al.* (2016), who had produced a blue precipitate with no typical nanoflower-like shape when there was no Cl$^-$ in reaction bulk, and by Ariza-Avidad and co-workers (2016), who have also found chlorine atoms in hNFs by EDS analysis [95,125].

Table 5 - Elemental composition of hybrid nanoflowers

Element	Cu^{2+}-hNF (Atom %)	Ca^{2+}-hNF (Atom %)
C-K	25.19	8.16
O-K	29.80	47.29
P-K	18.17	11.21
Cl-K	4.65	0.31
Cu-K	16.30	–
Ca-K	–	27.97

4.1.4 Fourier transform infrared spectroscopy

FTIR analysis was carried out to identify chemical structures and to prove the formation of organic-inorganic hybrid nanoflowers. The spectroscopy results are shown in Fig. 11. Characteristic bending vibrations of O=P—O were observed in ~560 cm^{-1} and ~630 cm^{-1} in both hybrids might be attributed to metal-phosphate groups in the structures [125,131]. The stretching bands 1400-1630 were attributed to NH$_2$ groups from peptide bonds [86]. Considerable peak weakening in 1020-1220 cm^{-1} and 1350-1470 cm^{-1} bands suggests changes in the secondary structure of the enzyme in the hybrid's formation [76]. The peaks perceived at 2800-3000 cm^{-1} are typical for CH$_2$ and CH$_3$ groups, while OH and NH groups stretching bands are found at ~3450 cm^{-1} [95,125]. Another significant absorption band, noticed in ~1090 cm^{-1}, might refer to the asymmetric vibration of Si—O [132].

This result is consistent with silica structures, observed in SEM analysis and characterized by EDS, in all samples tested. SEM images of those structures are presented in Fig. 12. Although the stabilizers used in the commercial enzyme are not specified, we were led to believe that silica compounds were present in the free enzyme sample for this purpose. Additionally, even in the presence of silica compounds, the hybrids' synthesis was not affected.

Figure 11 - FTIR of Ca^{2+}-hNF, Cu^{2+}-hNF, and free HRP
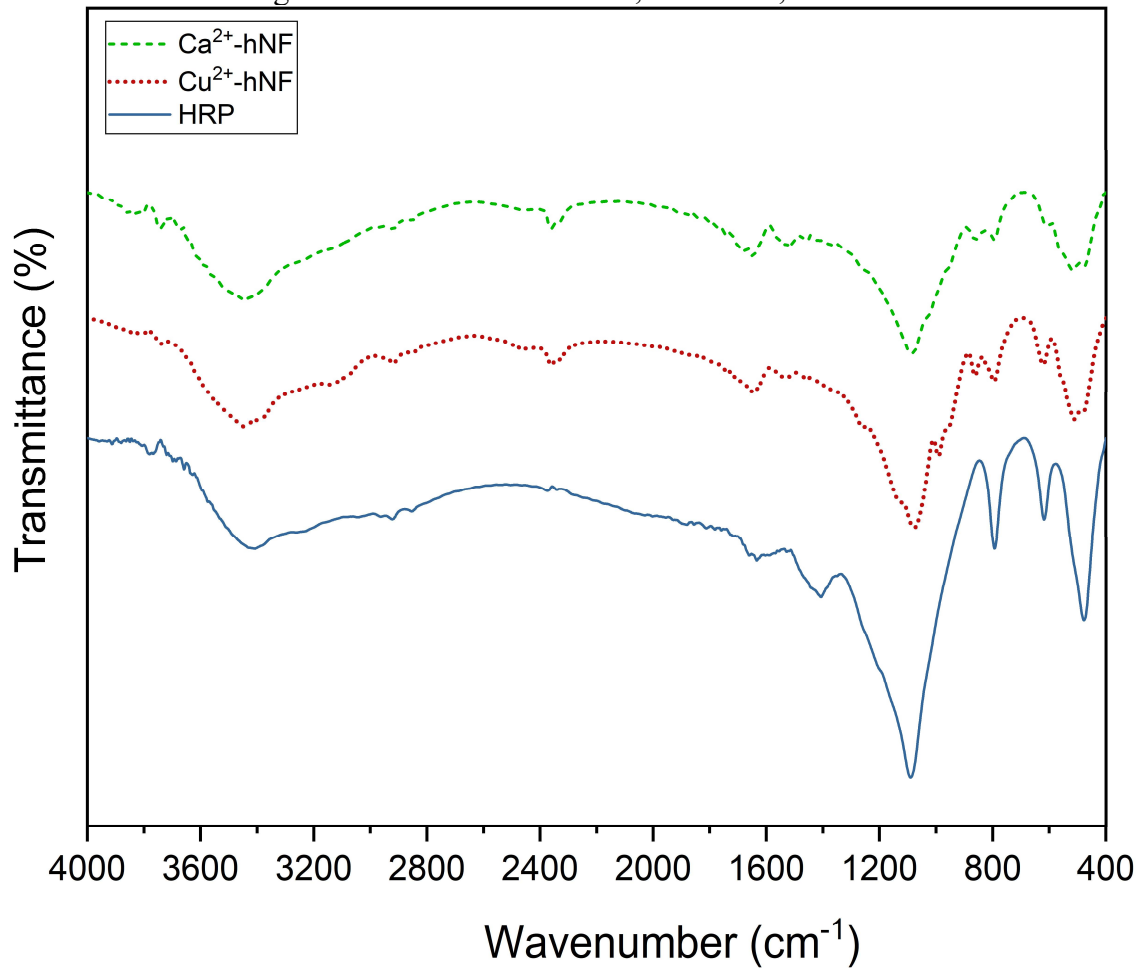
Figure 12 - SEM images of silica structures
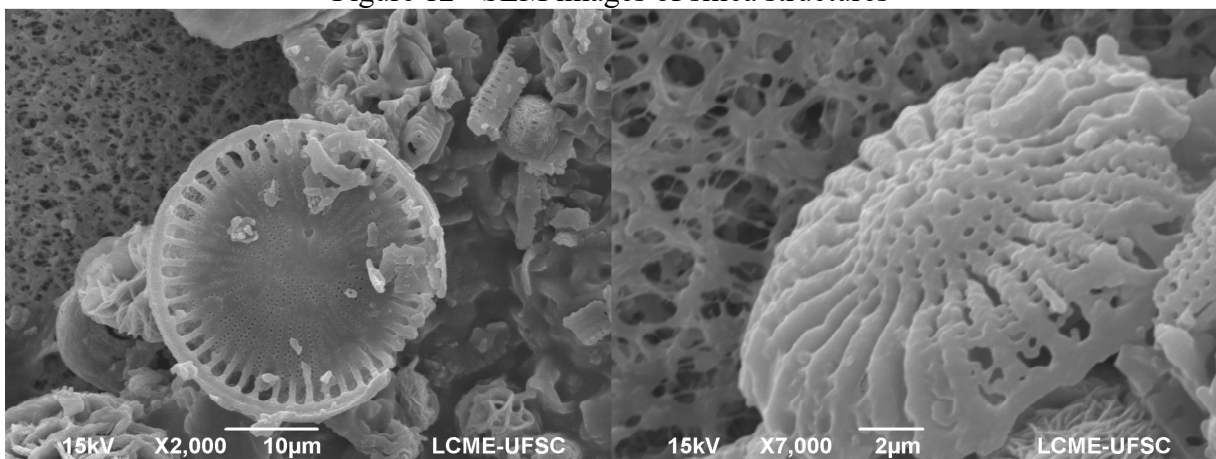
4.1.5 Powdered X-ray diffraction

XRD technique was employed to characterize the crystal phases of both hybrids, as presented in Fig. 13. XRD analysis has shown that copper hybrids (Fig. 13A) have peaks consistency with $Cu_3(PO_4)_2 \cdot 3H_2O$ crystals pattern (JCPDS No. 00-022-0548). This result is coherent with the previously reported synthesis of copper-enzyme hybrids [127,133–135]. Likewise, XRD of calcium hybrids (Fig. 13B) has exhibited correspondence with $Ca_3(PO_4)_2 \cdot 2H_2O$ (JCPDS No. 18-0303) and $CaHPO_4$ (JCPDS No. 9-80), both already communicated in earlier researches of calcium-enzyme structures [19,92].

It was also possible to visualize a major peak in both structures in $2\theta \approx 22$ °, referring to SiO_2 crystals (JCPDS No. 46-1045). This outcome confirms the presence of the structures seen in the preceding analysis carried out in this work.

Figure 13 - XRD spectrum of (A) Cu^{2+}-hNF and (B) Ca^{2+}-hNF
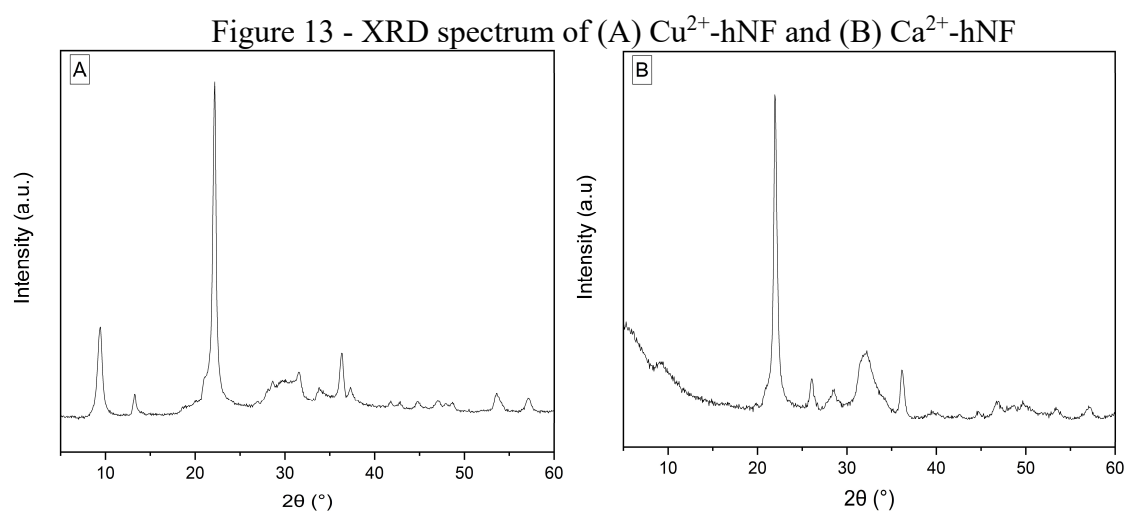
4.2 PH AND TEMPERATURE EFFECT ON THE ENZYME ACTIVITIES OF THE FREE HRP AND HNF PREPARATIONS

Optimal conditions of use for free HRP and hNFs were determined by activity assays. First, experiments to obtain the best pH were carried out at different pH values at room temperature. The results are reported in Fig. 14 as relative activity. The highest activity for each biocatalyst used was set as 100%, and other points were calculated as a fraction of this value. The optimal pH was 7.4, independently of the biocatalyst used. It shows that the hybrid formation of HRP with copper and calcium phosphates did not affect the enzyme's best pH value. Similar behaviors were detected by Rong *et al.* (2017) and by Memon *et al.* (2019),

where copper-enzyme and calcium-enzyme hybrids, respectively, presented the same best pH value that the free studied enzymes [16,92].

However, it is possible to notice that Cu^{2+}-hNF presents less activity loss with a pH increase from 9.0 to 12.0 than free HRP and Ca^{2+}-hNF. Previous works have also reported similar profiles in higher pH values for copper-enzyme hybrids than the free enzyme, suggesting greater enzyme stability within the tested conditions [75,121].

Figure 14 - Relative activity as a function of pH at 25 ºC for Cu^{2+}-hNF, Ca^{2+}-hNF, and free HRP
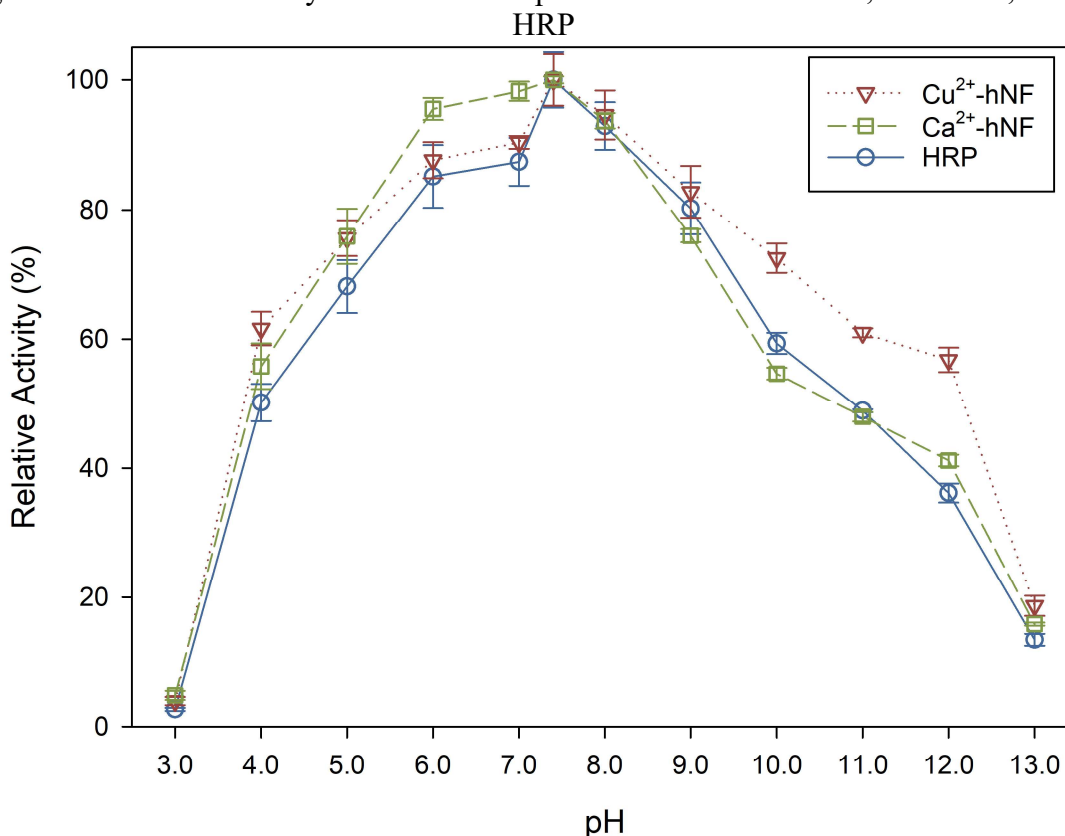
Subsequently, using the best pH value, activity was tested in different temperatures from 25 to 70 °C. The relative activity as a function of the highest activity for each biocatalyst is displayed in Fig. 15. As it happened with the pH evaluation, the synthesis of Cu^{2+}-hNFs and Ca^{2+}-hNFs did not affect the optimal temperature, detected to be 60 ºC for all cases. In parallel, hybrids prepared by Sun *et al.* (2014) and Wang *et al.* (2020) have maintained the optimal temperature of the free enzyme [18,94].

It was noticeable, though, that activity in both hybrids was less sensitive to temperature change in the range 25 to 40 °C than the free enzyme, which might represent an increase in the enzyme thermal robustness. At 70 °C, the activity losses compared to the highest values were

16.90%, 32.03%, 44.63% in Ca^{2+}-hNF, free-HRP, and Cu^{2+}-hNF, respectively. This higher activity in calcium hybrids might bespeak an advantage of these structures against the free enzyme and copper hybrids.

Figure 15 - Relative activity as a function of temperature in pH 7.4 for Cu^{2+}-hNF, Ca^{2+}-hNF, and free HRP
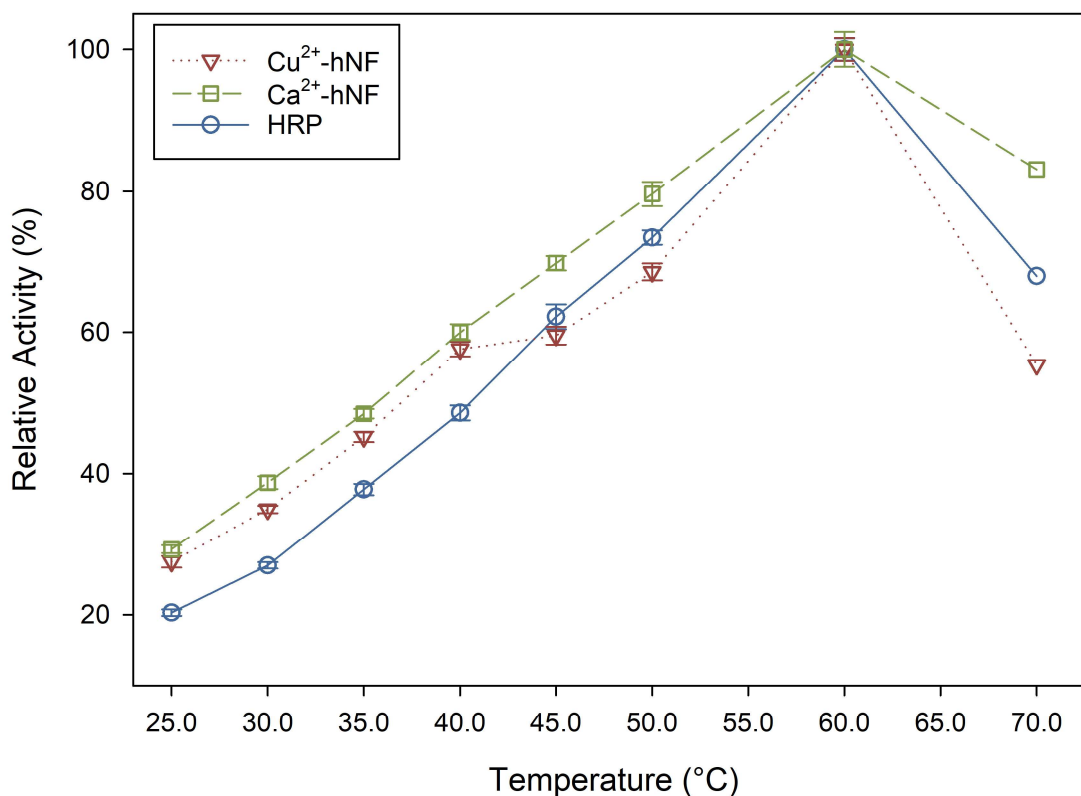
4.3 EFFECT OF PH AND TEMPERATURE ON STABILITY OF THE FREE HRP AND HNF PREPARATIONS

The effect of pH and temperature on the stability of the free enzyme and hybrid preparations was also investigated. All the results are expressed as relative activity, where the initial activity for each biocatalyst was set as 100%.

The pH stability was established with different buffer solutions: citrate buffer 0.1 M for pH 4.0 and 5.0; phosphate buffer for pH 6.0 and 7.4; Tris-HCl buffer 0.1 M for pH 8.0 and 9.0. According to the pH stability analysis (Fig. 16), in pH of 6.0 to 8.0 (Fig. 16C, 16D, and 16E), the free enzyme and hybrid preparations with copper and calcium showed similar deactivation profiles. Consequently, enzyme immobilization did not considerably affect the enzyme stability in those pH values. On the other hand, in pH of 9.0 (Fig. 16F), both hybrids presented discrete superior stability than the free form. In fact, after 24 h, copper and calcium hybrids maintained

97.97% and 96.38% of their initial activities, while free HRP kept 92.82% The smallest activity losses in 24 h of 5.51%, 6,49%, and 4,07% (free HRP, Cu^{2+}-hNF, and Ca^{2+}-hNF, respectively) were observed in the optimal pH 7.4.

However, calcium hybrids exhibited more significant deactivation in acid mediums than copper and free enzymes (Fig. 16A and 16B). This outcome suggests that hybrids' stability is completely related to their both organic and inorganic constituents. In this sense, conjugated polyketone reductase-calcium phosphate hybrids with sodium alginate coating prepared by Cheng *et al.* (2020) presented a notably smaller residual activity in acid mediums than free enzyme [136]. Consistently, Chen *et al.* (2018) have shown that, despite the higher activity of calcium-enzyme hybrids, the immobilized form of aldo-keto reductase (AKR) with calcium phosphate was more sensitive to acid pH changes than free enzyme [137]. In the same study, the authors have also noted that alcohol dehydrogenase (ADH) hybrids could keep the activity in the function of pH variance more easily, confirming the dependence of hybrid composition on their activity [137].

Figure 16 - Enzyme stability for Cu^{2+}-hNF, Ca^{2+}-hNF and free HRP in pH (A) 4.0, (B) 5.0, (C) 6.0, (D) 7.4, (E) 8.0, and (F) 9.0, at 25 ºC
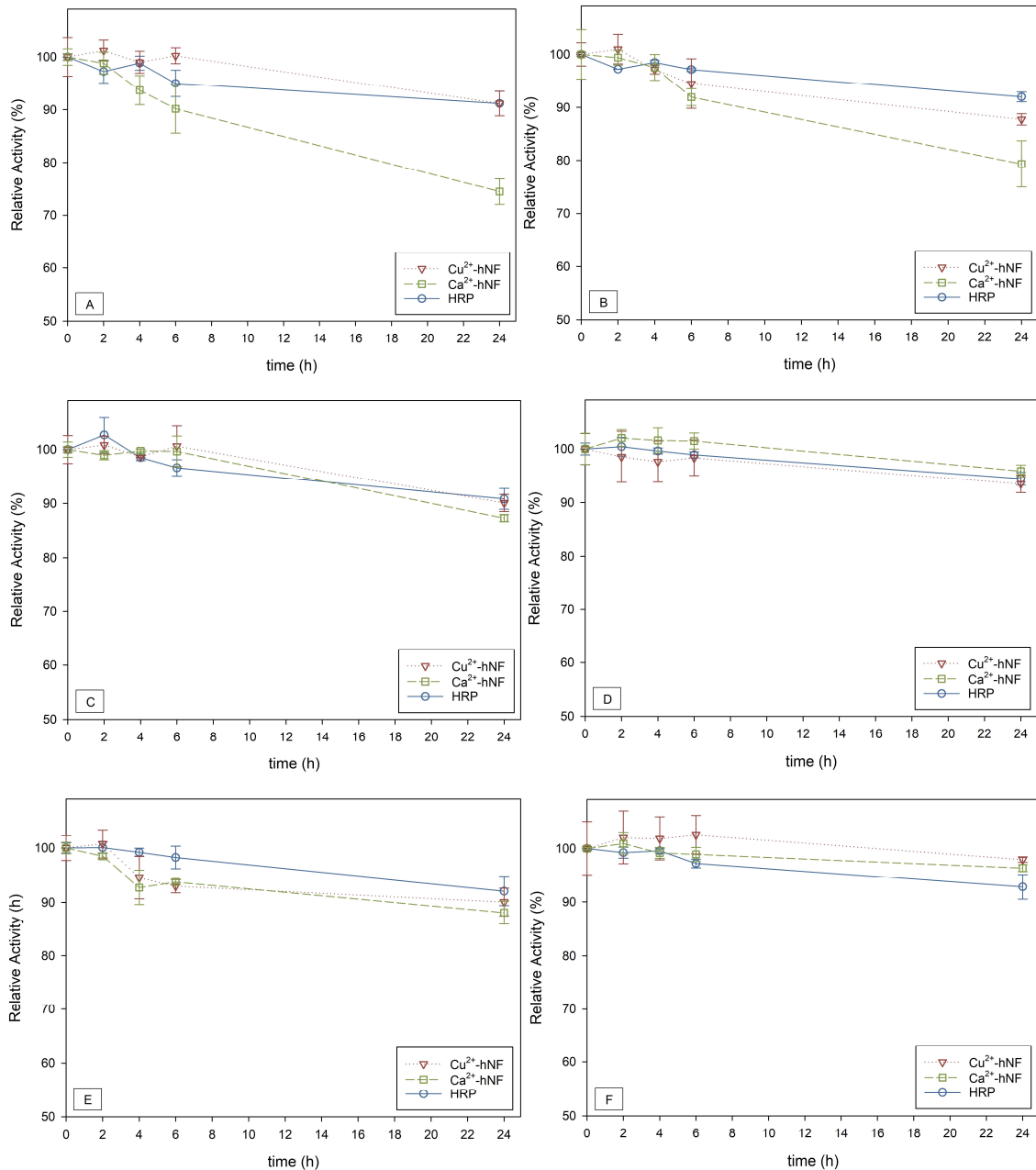
Thermal stability analysis indicated excellent stability for both hybrids and the free enzyme at 50 °C (Fig. 17A), where no considerable activity loss was seen within 8 h. At 60 °C (Fig. 17B), the optimal temperature for the enzyme activity, the residual activities after 8 h account for 79.61%, 76.61%, and 74.97% of the initial values for free HRP, copper, and calcium hybrids, respectively. Finally, at 70ºC (Fig. 17C), the favorable effect of the enzyme immobilization in copper hybrids in the stability is notable. While the free enzyme lost all its activity within 6 h, and copper hybrids showed only 5.59% of residual activity, calcium preparations were able to maintain 27.02% of its initial activity in this time and 26.42% in 8 h.

This result suggests a greater stability of HRP-calcium hybrids in higher temperatures. Analogously, Duan, Li, and Zhang (2018) have noted that metal-enzyme hybrids had greater thermal stability than free enzymes. Still, also calcium-enzyme tended to show the smallest activity loss in all temperature ranges, from 30 to 80 °C [138]. Chen and co-workers (2018) also presented improved thermal stabilities in calcium phosphate-enzyme hybrids within 8 h in temperatures ranging from 30 to 60 °C for both enzymes ADH and AKR. However, this stability upgrade was much more significant in AKR hybrids [137].

Figure 17 - Enzyme thermal stability for Cu^{2+}-hNF, Ca^{2+}-hNF, and free HRP in (A) 50 °C, (B) 60 °C, and (C) 70 °C, in pH 7.4
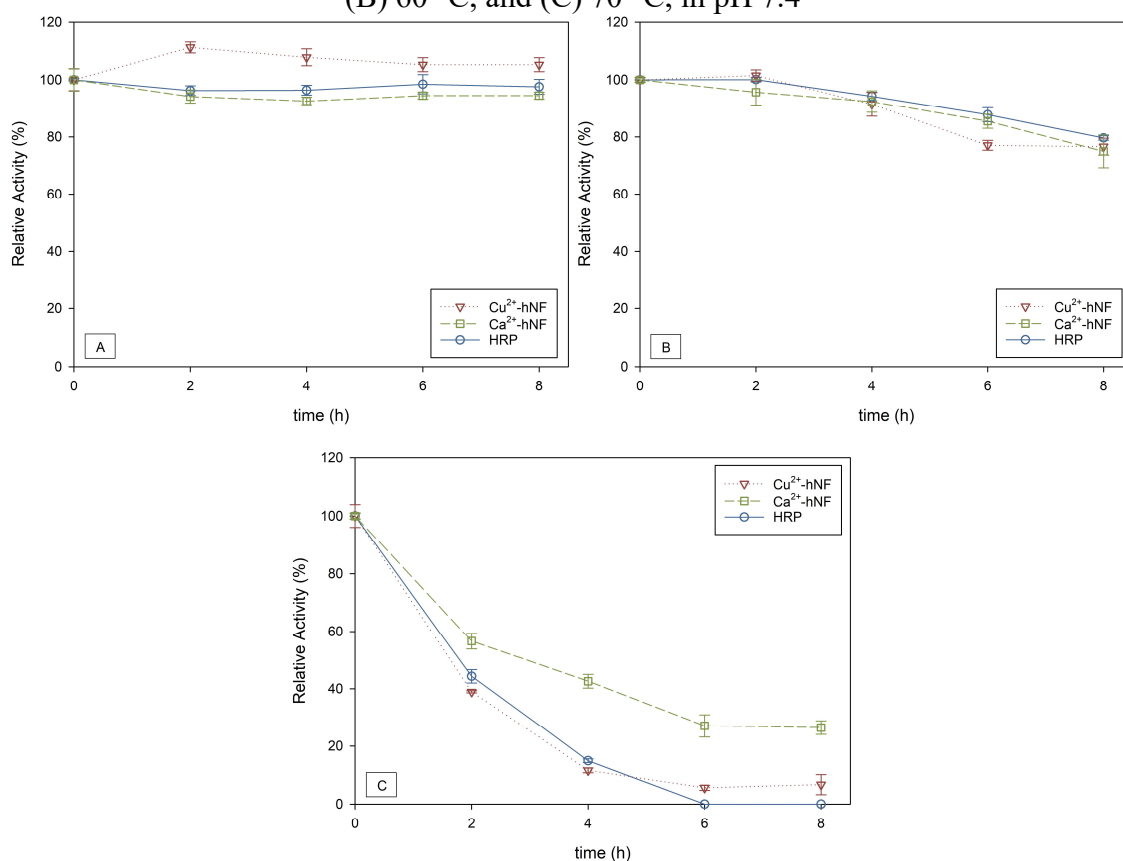
4.4 KINETIC PARAMETERS

A 10-step mechanism of the co-oxidation of phenols and 4-AAP, which includes quinonimine production, was proposed by Metelitza, Litvinchuk, and Savenkova (1991)[139]. However, even though the reaction has a complex mechanism, the initial reaction rate, as shown in Fig. 18, is a function of phenol concentration. This result suggests that, in the tested conditions, phenol consumption is the slow step of the mechanism, and it determines, consequently, the reaction rate. Although HRP immobilization into Ca^{2+}-hNF did not lead to a

considerable change in the kinetic profile of phenol consumption, Cu^{2+}-hNF seems to have had a substantial decrease in the maximum specific reaction rate.

Figure 18 – Initial specific reaction rates as a function of phenol concentration for Cu^{2+}-hNF, Ca^{2+}-hNF, and free HRP, pH 7.4 at 25 °C.*
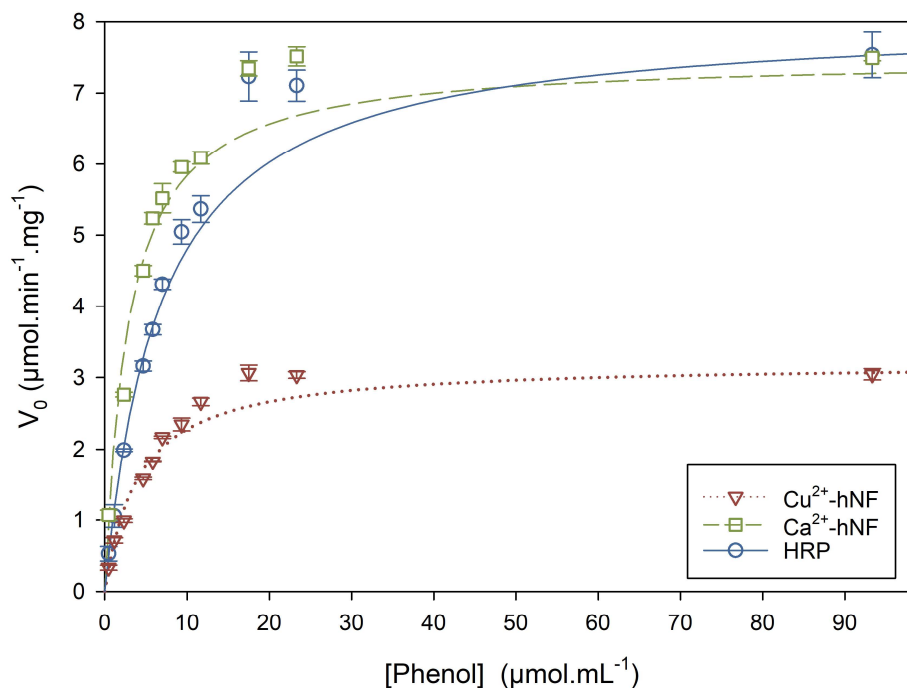
*Points represent average results of three independent experiments and error bars represent the respective standard deviations. Curves represent the Michaelis-Menten model fitting to the data for each biocatalyst tested.

A double reciprocal plot, which can be visualized in Fig. 19, was finally produced to determine the kinetic parameters K_M, V_{max}, and k_{cat} (Table 6) and quantify those differences after immobilization. Excellent model fitting to the experimental data, evidenced by parameter R^2 equal to 0.994, 0.995, and 0.990 for free-HRP, copper, and calcium hybrids, respectively, indicates the validity of the method approximation.

Figure 19 - Lineweaver-Burk plot for Cu^{2+}-hNF, Ca^{2+}-hNF, and free HRP
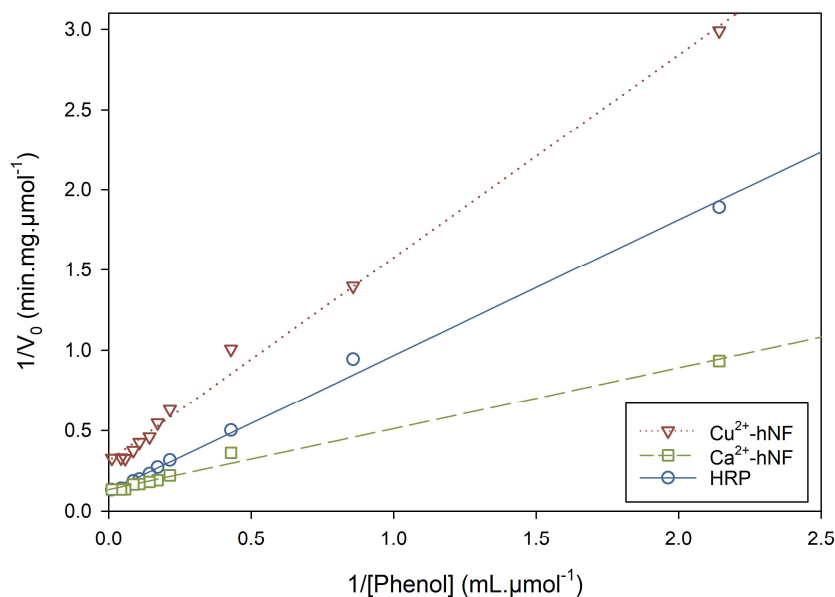
The Michaelis constant K_M value indicates the affinity of the enzyme active sites towards the substrate, in this case, phenol. Smaller values of K_M represent greater affinity. The K_M was 6.82 $\mu mol.mL^{-1}$ in free enzyme, 4.05 $\mu mol.mL^{-1}$ in copper hybrids, and 2.84 $\mu mol.mL^{-1}$ in calcium hybrids. This outcome suggests that both hybrids, especially calcium ones, have more affinity to the substrate than free enzyme, favoring the reaction.

However, despite superior stability in binding enzyme-substrate after immobilization, V_{max} was not increased for either hybrid compared to the free enzyme. In fact, the value did not present considerable change from 8.08 $\mu mol.min^{-1}.mg^{-1}$ in free enzyme to 7.50 $\mu mol.min^{-1}.mg^{-1}$ in calcium hybrids, although this value decreased to 3.20 $\mu mol.min^{-1}.mg^{-1}$ in Cu^{2+}-hNF. Correspondingly, magnetic-activated lipase-inorganic hybrid nanoflowers prepared by Zhong *et al.* (2021) have also presented smaller K_M, and V_{max} values than the free enzyme, evidencing a deeper affinity between the enzyme and the substrate does not necessarily induce a higher reaction rate [140].

The turnover number, or k_{cat}, representing the frequency of substrate molecules converted into products by one enzyme molecule, remained similar in calcium hybrids and decreased considerably in copper hybrids compared to the free enzyme. Nevertheless, k_{cat}/K_M value was 2.23 times higher in calcium hybrids than in the free enzyme, indicating that immobilization of free HRP into these hybrids might lead to a higher enzymatic efficiency. Zhang *et al.* (2020) reported similar kinetic results by using a lipase as the organic portion. The authors have shown that catalytic efficiency was greater for calcium hybrids and smaller for copper hybrids. At the same time, K_M was lower for both calcium and copper hybrids compared

to the values for the free enzyme [19]. A 2.2-fold higher catalytic efficiency than the free enzyme was equally described by Patel *et al.* (2018), employing copper-laccase nanoflowers cross-linked with glutaraldehyde [17].

Table 6 - Kinetic parameters of Cu^{2+}-hNF, Ca^{2+}-hNF, and free HRP

Biocatalyst form	K_M ($\mu mol.mL^{-1}$)	V_{max} ($\mu mol.min^{-1}.mg^{-1}$)	k_{cat} (s^{-1})	k_{cat}/K_M ($s^{-1}.mM^{-1}$)
free-HRP	6.82 ± 0.87	8.08 ± 0.92	5.92 ± 0.67	0.87 ± 0.21
Cu^{2+}-hNF	4.05 ± 0.36	3.20 ± 0.23	2.34 ± 0.17	0.58 ± 0.09
Ca^{2+}-hNF	2.84 ± 0.26	7.50 ± 0.52	5.49 ± 0.38	1.93 ± 0.31

4.5 MEMBRANE-BASED PHENOL BIOSENSING

The membrane-based biosensors, produced onto PVDF hydrophilic membranes with a pore size of 0.22 μm, were tested with 50 μL of a sample, with pH 7.4, containing H_2O_2 0.88 $\mu mol.mL^{-1}$, 4-AAP 1.1 $\mu mol.mL^{-1}$ and phenol concentrations of 24.00, 19.20, 14.40, 9.60, 4.80, 2.40, 1.44, 0.96 and 0.72 $\mu mol.mL^{-1}$ (Fig. 20A-J, respectively). Fig. 20 shows the biosensors produced with (1) free HRP, (2) Cu^{2+}-hNF, and (3) Ca^{2+}-hNF after 1 min of reaction time at 25 °C. Three measurements were performed to each phenol concentration in all biosensors to confirm the results.

Both biosensors produced with HRP-copper and HRP-calcium hybrids effectively detected phenol ranging from 0.72 to 24.00 $\mu mol.mL^{-1}$. Although color change seems greater in calcium hybrids at higher phenol concentrations, as can be seen in Fig. 20A, probably due to their higher catalytic efficiency, both calcium and copper biosensors showed similar performance for phenol detection within the concentration range tested. Control biosensors, produced with an equivalent amount of free enzyme (Fig. 20-1), did not present any considerable color switch in none of the phenol concentrations tested. It might have occurred due to enzyme spread through the membrane pores, attenuating visible changes.

As expected, it was noticeable in metal-HRP hybrid biosensors that the pink color softened with the decreasing phenol concentration. The smallest concentration of phenol where it was possible to detect the visible color change under the experimental conditions was 0.72 $\mu mol.mL^{-1}$. Below this concentration, no color was seen in any of the biosensors within 1 min.

A colorimetric method for phenol sensing using copper-laccase nanoflowers developed by Zhu *et al.* (2013) detected phenol in a similar range from 0.4 to 50 $\mu mol.mL^{-1}$. However,

those results were obtained in a higher reaction time of 5 minutes [35]. Another phenol biosensing using enzyme-inorganic hybrids was described by Lin *et al.* (2014). Even though the authors have achieved an excellent detection limit (LOD) of 1.0 μM, the method uses greater sample volume, hybrids amount, and reaction time [42].

A typical synthesis of hybrid nanoflowers following the methodology described in the present work uses only 2.5 mg of HRP and can produce up to 200 units of phenol detection. It might evidence a simple, low-cost, and efficient approach to assemble qualitative enzymatic biosensors for a rapid phenol detection in concentrations up from 0.72 $\mu mol.mL^{-1}$. The simplicity of this approach might also represent greater viability to a fast *in situ* analysis to determine the presence of phenol in the environment.

Figure 20 - Images of the biosensors produced with (1) free-HRP, (2) Cu^{2+}-hNF and (3) Ca^{2+}-hNF after 1 min reaction with different initial concentrations of phenol of (A) 24.00, (B) 19.20, (C) 14.40, (D) 9.60, (E) 4.80, (F) 2.40, (G) 1.92, (H) 1.44, (I) 0.96, and (J) 0.72 μmol.mL^{-1}.
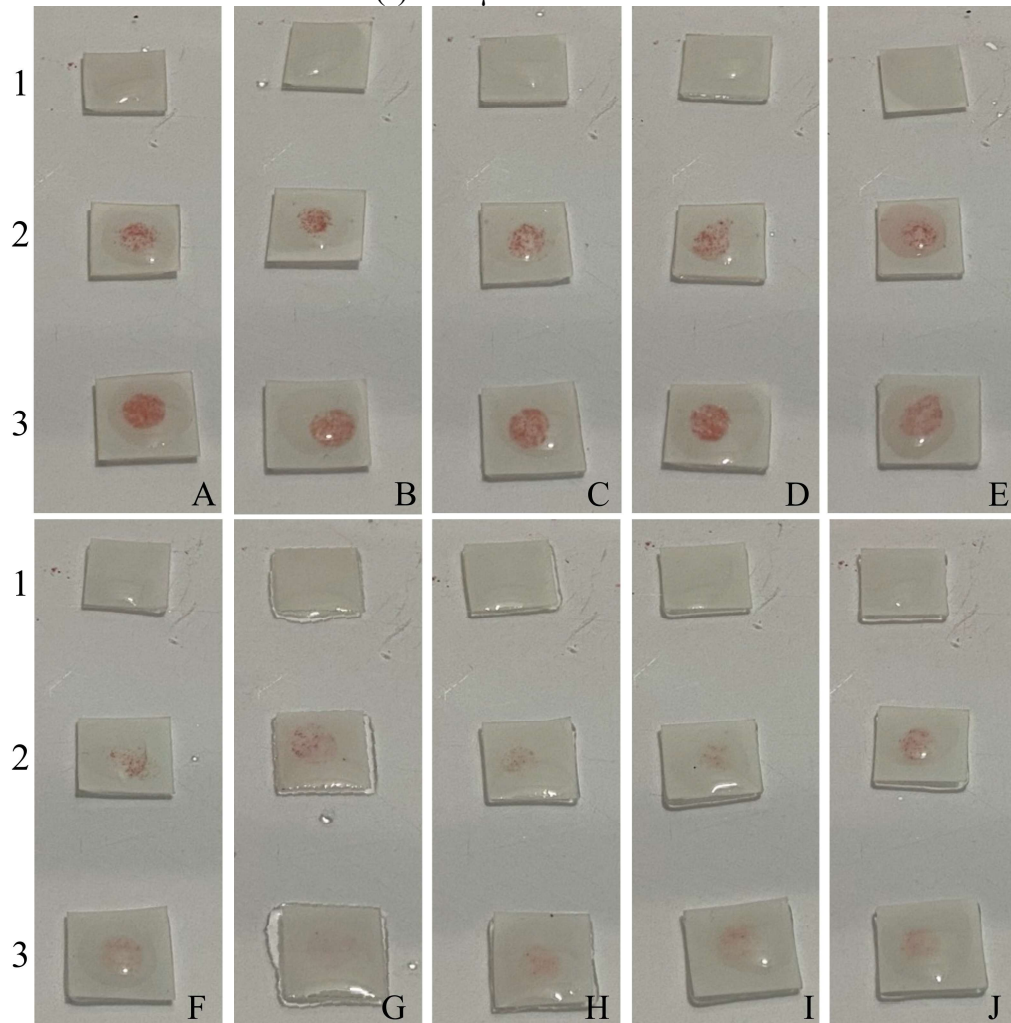
5 CONCLUSIONS

In summary, a simple, rapid, and low-cost, qualitative biosensor for visual detection of phenol using copper-HRP and calcium-HRP hybrid nanoflowers was successfully developed. Both biosensors, prepared with copper and calcium hybrids, could detect phenol in concentrations ranging from 0.72 μmol.mL^{-1} to 24.00 μmol.mL^{-1} in 1 min of reaction time.

The highest encapsulation yield values, 92.3% and 92.0%, were obtained for copper and calcium hybrids, respectively, using the best enzyme concentration of 0.25 mg.mL^{-1} in the synthesis medium. With this enzyme concentration, copper nanoflowers presented a good morphology. Calcium hybrids, however, did not exhibit a flower-like form within the same conditions, evidencing that both enzyme concentration and metal ion type are essential to define the enzyme-inorganic structure.

Despite the divergence in hybrid morphologies depending on the ion used in their synthesis, Cu^{2+}-hNF and Ca^{2+}-hNF proper formation was confirmed by EDS, FTIR, and XRD analysis. For all the biocatalyst forms tested, the best pH and temperature values were 7.4 and 60 °C, respectively.

Both hybrids have presented great stability in pH from 4.0 to 9.0, similar to the free enzyme. Further, all the biocatalysts tested demonstrated excellent thermal stability at 50 °C, and similar deactivation profiles at 60 °C. At 70° C, the favorable effect of enzyme immobilization into Ca^{2+}-hNF was noted since these hybrids were able to maintain their activity for longer periods.

In addition, kinetic parameters were determined. K_M constant decreased from 6.82 μmol.mL^{-1} in the free enzyme to 4.05 μmol.mL^{-1} and 2.84 μmol.mL^{-1}, in Cu^{2+}-hNF and Ca^{2+}-hNF, respectively. Moreover, Ca^{2+}-hNF presented a k_{cat}/K_M value 2.23 times higher than the free HRP, indicating that immobilizing the free enzyme into calcium hybrids might increase enzymatic efficiency.

Furthermore, up to 200 units of biosensors can be produced using only 2.5 mg of HRP with the approach described in the present work. Considering all the facts disclosed above, we believe that the developed biosensors can be a helpful tool in practical and rapid *in situ* phenol detection.

Although a small amount of enzyme was used to prepare each biosensor, the reusability of the formed biosensors was not tested in this study. It might be, then, an interesting approach for a future work. Another subject that might also be explored is the efficiency of this biosensor using real samples for phenol detection, considering their color and the presence of other

chemicals. Finally, the hybrid synthesis yield might also be examined to obtain a higher production of nanoflowers in each batch.

REFERENCES

[1]   Li X, Li S, Liang X, McClements DJ, Liu X, Liu F. Applications of oxidases in modification of food molecules and colloidal systems: Laccase, peroxidase and tyrosinase. Trends Food Sci Technol 2020;103:78–93. https://doi.org/10.1016/j.tifs.2020.06.014.

[2]   Zhu Y, Tao H, Janaswamy S, Zou F, Cui B, Guo L. The functionality of laccase- or peroxidase-treated potato flour: Role of interactions between protein and protein/starch. Food Chem 2021;341:128082. https://doi.org/10.1016/j.foodchem.2020.128082.

[3]   Bagheri pebdeni A, Hosseini M. Fast and selective whole cell detection of Staphylococcus aureus bacteria in food samples by paper based colorimetric nanobiosensor using peroxidase-like catalytic activity of DNA-Au/Pt bimetallic nanoclusters. Microchem J 2020;159:105475. https://doi.org/10.1016/j.microc.2020.105475.

[4]   Touahar IE, Haroune L, Ba S, Bellenger JP, Cabana H. Characterization of combined cross-linked enzyme aggregates from laccase, versatile peroxidase and glucose oxidase, and their utilization for the elimination of pharmaceuticals. Sci Total Environ 2014;481:90–9. https://doi.org/10.1016/j.scitotenv.2014.01.132.

[5]   Poliakov AE, Dumshakova A V., Muginova S V., Shekhovtsova TN. A peroxidase-based method for the determination of dopamine, adrenaline, and α-methyldopa in the presence of thyroid hormones in pharmaceutical forms. Talanta 2011;84:710–6. https://doi.org/10.1016/j.talanta.2011.01.074.

[6]   Na SY, Lee Y. Elimination of trace organic contaminants during enhanced wastewater treatment with horseradish peroxidase/hydrogen peroxide (HRP/H2O2) catalytic process. Catal Today 2017;282:86–94. https://doi.org/10.1016/j.cattod.2016.03.049.

[7]   Al-Dhabi NA, Esmail GA, Valan Arasu M. Effective degradation of tetracycline by manganese peroxidase producing Bacillus velezensis strain Al-Dhabi 140 from Saudi Arabia using fibrous-bed reactor. Chemosphere 2021;268:128726. https://doi.org/10.1016/j.chemosphere.2020.128726.

[8]   Yadav N, Govindwar SP, Rane N, Ahn H-J, Xiong J-Q, Jang M, et al. Insights on the role of periphytic biofilm in synergism with Iris pseudacorus for removing mixture of pharmaceutical contaminants from wastewater. J Hazard Mater 2021;418:126349. https://doi.org/10.1016/j.jhazmat.2021.126349.

[9]   Garg S, Kumar P, Singh S, Yadav A, Dumée LF, Sharma RS, et al. Prosopis juliflora peroxidases for phenol remediation from industrial wastewater — An innovative practice for environmental sustainability. Environ Technol Innov 2020;19:100865. https://doi.org/10.1016/j.eti.2020.100865.

[10]   Darwesh OM, Matter IA, Eida MF. Development of peroxidase enzyme immobilized magnetic nanoparticles for bioremediation of textile wastewater dye. J Environ Chem Eng 2019;7:102805. https://doi.org/10.1016/j.jece.2018.11.049.

[11]   de Oliveira FK, Santos LO, Buffon JG. Mechanism of action, sources, and application of peroxidases. Food Res Int 2021;143:110266.

https://doi.org/10.1016/j.foodres.2021.110266.

[12] Sheldon RA, van Pelt S. Enzyme immobilisation in biocatalysis: Why, what and how. Chem Soc Rev 2013;42:6223–35. https://doi.org/10.1039/c3cs60075k.

[13] Ge J, Lei J, Zare RN. Protein-inorganic hybrid nanoflowers. Nat Nanotechnol 2012;7:428–32. https://doi.org/10.1038/nnano.2012.80.

[14] Maurya SS, Nadar SS, Rathod VK. Dual activity of laccase-lysine hybrid organic–inorganic nanoflowers for dye decolourization. Environ Technol Innov 2020;19:100798. https://doi.org/10.1016/j.eti.2020.100798.

[15] Wang S, Ding Y, Chen R, Hu M, Li S, Zhai Q, et al. Multilayer petal-like enzymatic-inorganic hybrid micro-spheres [CPO-(Cu/Co/Cd)3(PO4)2] with high bio-catalytic activity. Chem Eng Res Des 2018;134:52–61. https://doi.org/10.1016/j.cherd.2018.03.036.

[16] Rong J, Zhang T, Qiu F, Zhu Y. Preparation of Efficient, Stable, and Reusable Laccase-Cu 3 (PO 4) 2 Hybrid Microspheres Based on Copper Foil for Decoloration of Congo Red. ACS Sustain Chem Eng 2017;5:4468–77. https://doi.org/10.1021/acssuschemeng.7b00820.

[17] Patel SKS, Otari S V., Li J, Kim DR, Kim SC, Cho BK, et al. Synthesis of cross-linked protein-metal hybrid nanoflowers and its application in repeated batch decolorization of synthetic dyes. J Hazard Mater 2018;347:442–50. https://doi.org/10.1016/j.jhazmat.2018.01.003.

[18] Wang A, Chen X, Yu J, Li N, Li H, Yin Y, et al. Green preparation of lipase@Ca3(PO4)2 hybrid nanoflowers using bone waste from food production for efficient synthesis of clindamycin palmitate. J Ind Eng Chem 2020;89:383–91. https://doi.org/10.1016/j.jiec.2020.06.007.

[19] Zhang Y, Sun W, Elfeky NM, Wang Y, Zhao D, Zhou H, et al. Self-assembly of lipase hybrid nanoflowers with bifunctional Ca2+ for improved activity and stability. Enzyme Microb Technol 2020;132:109408. https://doi.org/10.1016/j.enzmictec.2019.109408.

[20] He X, Chen L, He Q, Xiao H, Zhou X, Ji H. Cytochrome P450 Enzyme-Copper Phosphate Hybrid Nano-Flowers with Superior Catalytic Performances for Selective Oxidation of Sulfides. Chinese J Chem 2017;35:693–8. https://doi.org/10.1002/cjoc.201600714.

[21] Li WY, Lu SY, Bao SJ, Shi ZZ, Lu Z, Li CM, et al. Efficient in situ growth of enzyme-inorganic hybrids on paper strips for the visual detection of glucose. Biosens Bioelectron 2018;99:603–11. https://doi.org/10.1016/j.bios.2017.08.015.

[22] Cheon HJ, Adhikari MD, Chung M, Tran TD, Kim J, Kim M Il. Magnetic Nanoparticles-Embedded Enzyme-Inorganic Hybrid Nanoflowers with Enhanced Peroxidase-Like Activity and Substrate Channeling for Glucose Biosensing. Adv Healthc Mater 2019;8:1–8. https://doi.org/10.1002/adhm.201801507.

[23] Batule BS, Park KS, Gautam S, Cheon HJ, Kim M Il, Park HG. Intrinsic peroxidase-like activity of sonochemically synthesized protein copper nanoflowers and its application for the sensitive detection of glucose. Sensors Actuators, B Chem 2019;283:749–54. https://doi.org/10.1016/j.snb.2018.12.028.

[24] Zhang M, Yang N, Liu Y, Tang J. Synthesis of catalase-inorganic hybrid nanoflowers via sonication for colorimetric detection of hydrogen peroxide. Enzyme Microb Technol 2019;128:22–5. https://doi.org/10.1016/j.enzmictec.2019.04.016.

[25] Altinkaynak C, Yilmaz I, Koksal Z, Özdemir H, Ocsoy I, Özdemir N. Preparation of lactoperoxidase incorporated hybrid nanoflower and its excellent activity and stability. Int J Biol Macromol 2016;84:402–9. https://doi.org/10.1016/j.ijbiomac.2015.12.018.

[26] Ye R, Zhu C, Song Y, Song J, Fu S, Lu Q, et al. One-pot bioinspired synthesis of all-inclusive protein-protein nanoflowers for point-of-care bioassay: Detection of: E. coli O157:H7 from milk. Nanoscale 2016;8:18980–6. https://doi.org/10.1039/c6nr06870g.

[27] Gay NH, Phopin K, Suwanjang W, Songtawee N, Ruankham W, Wongchitrat P, et al. Neuroprotective Effects of Phenolic and Carboxylic Acids on Oxidative Stress-Induced Toxicity in Human Neuroblastoma SH-SY5Y Cells. Neurochem Res 2018;43:619–36. https://doi.org/10.1007/s11064-017-2463-x.

[28] Jun LY, Yon LS, Mubarak NM, Bing CH, Pan S, Danquah MK, et al. An overview of immobilized enzyme technologies for dye and phenolic removal from wastewater. J Environ Chem Eng 2019;7:102961. https://doi.org/10.1016/j.jece.2019.102961.

[29] Arciuli M, Palazzo G, Gallone A, Mallardi A. Bioactive paper platform for colorimetric phenols detection. Sensors Actuators, B Chem 2013;186:557–62. https://doi.org/10.1016/j.snb.2013.06.042.

[30] Guan Y, Liu L, Chen C, Kang X, Xie Q. Effective immobilization of tyrosinase via enzyme catalytic polymerization of L-DOPA for highly sensitive phenol and atrazine sensing. Talanta 2016;160:125–32. https://doi.org/10.1016/j.talanta.2016.07.003.

[31] Abdullah J, Ahmad M, Karuppiah N, Heng LY, Sidek H. Immobilization of tyrosinase in chitosan film for an optical detection of phenol. Sensors Actuators, B Chem 2006;114:604–9. https://doi.org/10.1016/j.snb.2005.06.019.

[32] Hashim HS, Fen YW, Sheh Omar NA, Abdullah J, Daniyal WMEMM, Saleviter S. Detection of phenol by incorporation of gold modified-enzyme based graphene oxide thin film with surface plasmon resonance technique. Opt Express 2020;28:9738. https://doi.org/10.1364/oe.387027.

[33] Wen Y, Li R, Liu J, Zhang X, Wang P, Zhang X, et al. Promotion effect of Zn on 2D bimetallic NiZn metal organic framework nanosheets for tyrosinase immobilization and ultrasensitive detection of phenol. Anal Chim Acta 2020;1127:131–9. https://doi.org/10.1016/j.aca.2020.06.062.

[34] Zhang S, Zhao H, John R. A dual-phase biosensing system for the determination of phenols in both aqueous and organic media. Anal Chim Acta 2001;441:95–105. https://doi.org/10.1016/S0003-2670(01)01079-0.

[35] Zhu L, Gong L, Zhang Y, Wang R, Ge J, Liu Z, et al. Rapid detection of phenol using a membrane containing laccase nanoflowers. Chem - An Asian J 2013;8:2358–60. https://doi.org/10.1002/asia.201300020.

[36] Casero E, Petit-Domínguez MD, Vázquez L, Ramírez-Asperilla I, Parra-Alfambra AM, Pariente F, et al. Laccase biosensors based on different enzyme immobilization strategies for phenolic compounds determination. Talanta 2013;115:401–8.

https://doi.org/10.1016/j.talanta.2013.05.045.

[37] Roy JJ, Abraham TE, Abhijith KS, Kumar PVS, Thakur MS. Biosensor for the determination of phenols based on Cross-Linked Enzyme Crystals (CLEC) of laccase. Biosens Bioelectron 2005;21:206–11. https://doi.org/10.1016/j.bios.2004.08.024.

[38] Othman AM, Wollenberger U. Amperometric biosensor based on coupling aminated laccase to functionalized carbon nanotubes for phenolics detection. Int J Biol Macromol 2020;153:855–64. https://doi.org/10.1016/j.ijbiomac.2020.03.049.

[39] Jarosz-Wilkołazka A, Ruzgas T, Gorton L. Amperometric detection of mono- and diphenols at Cerrena unicolor laccase-modified graphite electrode: Correlation between sensitivity and substrate structure. Talanta 2005;66:1219–24. https://doi.org/10.1016/j.talanta.2005.01.026.

[40] Cho SH, Shim J, Yun SH, Moon SH. Enzyme-catalyzed conversion of phenol by using immobilized horseradish peroxidase (HRP) in a membraneless electrochemical reactor. Appl Catal A Gen 2008;337:66–72. https://doi.org/10.1016/j.apcata.2007.11.038.

[41] Rosatto SS, Sotomayor PT, Kubota LT, Gushikem Y. SiO2/Nb2O5 sol-gel as a support for HRP immobilization in biosensor preparation for phenol detection. Electrochim Acta 2002;47:4451–8. https://doi.org/10.1016/S0013-4686(02)00516-9.

[42] Lin Z, Xiao Y, Yin Y, Hu W, Liu W, Yang H. Facile synthesis of enzyme-inorganic hybrid nanoflowers and its application as a colorimetric platform for visual detection of hydrogen peroxide and phenol. ACS Appl Mater Interfaces 2014;6:10775–82. https://doi.org/10.1021/am502757e.

[43] Ozoner SK, Keskinler B, Erhan E. HRP immobilized microporous Poly(styrene-divinylbenzene-polyglutaraldehyde) monolith for forced flow injected phenol biosensing. Mater Sci Eng C 2011;31:663–8. https://doi.org/10.1016/j.msec.2010.12.018.

[44] Rahemi V, Trashin S, Hafideddine Z, Meynen V, Van Doorslaer S, De Wael K. Enzymatic sensor for phenols based on titanium dioxide generating surface confined ROS after treatment with H2O2. Sensors Actuators, B Chem 2019;283:343–8. https://doi.org/10.1016/j.snb.2018.12.039.

[45] Çevik E, Şenel M, Baykal A, Abasiyanik MF. A novel amperometric phenol biosensor based on immobilized HRP on poly(glycidylmethacrylate)-grafted iron oxide nanoparticles for the determination of phenol derivatives. Sensors Actuators, B Chem 2012;173:396–405. https://doi.org/10.1016/j.snb.2012.07.026.

[46] Yang S, Chen Z, Jin X, Lin X. HRP biosensor based on sugar-lectin biospecific interactions for the determination of phenolic compounds. Electrochim Acta 2006;52:200–5. https://doi.org/10.1016/j.electacta.2006.04.059.

[47] Basso A, Serban S. Industrial applications of immobilized enzymes—A review. Mol Catal 2019;479:110607. https://doi.org/10.1016/j.mcat.2019.110607.

[48] Griengl H, Schwab H, Fechter M. The synthesis of chiral cyanohydrins by oxynitrilases. Trends Biotechnol 2000;18:252–6. https://doi.org/10.1016/S0167-7799(00)01452-9.

[49] Rubin-Pitel S, Zhao H. Recent Advances in Biocatalysis by Directed Enzyme Evolution. Comb Chem High Throughput Screen 2006;9:247–57. https://doi.org/10.2174/138620706776843183.

[50] Mendes AA. Seleção de suportes e protocolos de imobilização de lipases para a síntese enzimática de biodiesel. Universidade Fedeal de São Carlos, 2009.

[51] De Castro HF, Mendes AA, Dos Santos JC, De Aguiar CL. Modificação de óleos e gorduras por biotransformação. Quim Nova 2004;27:146–56. https://doi.org/10.1590/s0100-40422004000100025.

[52] Datta S, Christena LR, Rajaram YRS. Enzyme immobilization: an overview on techniques and support materials. 3 Biotech 2013;3:1–9. https://doi.org/10.1007/s13205-012-0071-7.

[53] Mateo C, Palomo JM, Fernandez-Lorente G, Guisan JM, Fernandez-Lafuente R. Improvement of enzyme activity, stability and selectivity via immobilization techniques. Enzyme Microb Technol 2007;40:1451–63. https://doi.org/10.1016/j.enzmictec.2007.01.018.

[54] Mehta J, Bhardwaj N, Bhardwaj SK, Kim KH, Deep A. Recent advances in enzyme immobilization techniques: Metal-organic frameworks as novel substrates. Coord Chem Rev 2016;322:30–40. https://doi.org/10.1016/j.ccr.2016.05.007.

[55] Altinkaynak C, Tavlasoglu S, Özdemir N, Ocsoy I. A new generation approach in enzyme immobilization: Organic-inorganic hybrid nanoflowers with enhanced catalytic activity and stability. Enzyme Microb Technol 2016;93–94:105–12. https://doi.org/10.1016/j.enzmictec.2016.06.011.

[56] Cipolatti EP, Valério A, Henriques RO, Moritz DE, Ninow JL, Freire DMG, et al. Nanomaterials for biocatalyst immobilization-state of the art and future trends. RSC Adv 2016;6:104675–92. https://doi.org/10.1039/c6ra22047a.

[57] Wu X, Hou M, Ge J. Metal-organic frameworks and inorganic nanoflowers: A type of emerging inorganic crystal nanocarrier for enzyme immobilization. Catal Sci Technol 2015;5:5077–85. https://doi.org/10.1039/c5cy01181g.

[58] Schärtl W. Crosslinked spherical nanoparticles with core-shell topology. Adv Mater 2000;12:1899–908. https://doi.org/10.1002/1521-4095(200012)12:24<1899::AID-ADMA1899>3.0.CO;2-T.

[59] Park KS, Batule BS, Chung M, Kang KS, Park TJ, Kim M Il, et al. A simple and eco-friendly one-pot synthesis of nuclease-resistant DNA-inorganic hybrid nanoflowers. J Mater Chem B 2017;5:2231–4. https://doi.org/10.1039/c6tb03047e.

[60] Ye R, Zhu C, Song Y, Lu Q, Ge X, Yang X, et al. Bioinspired synthesis of all-in-one organic–inorganic hybrid nanoflowers combined with a handheld pH meter for on-site detection of food pathogen. Small 2016;12:3094–100. https://doi.org/10.1002/smll.201600273.

[61] Fang Y, Wang S, Liu Y, Xu Z, Zhang K, Guo Y. Development of Cu nanoflowers modified the flexible needle-type microelectrode and its application in continuous monitoring glucose in vivo. Biosens Bioelectron 2018;110:44–51. https://doi.org/10.1016/j.bios.2018.03.024.

[62]   He L, Zhang S, Ji H, Wang M, Peng D, Yan F, et al. Protein-templated cobaltous phosphate nanocomposites for the highly sensitive and selective detection of platelet-derived growth factor-BB. Biosens Bioelectron 2016;79:553–60. https://doi.org/10.1016/j.bios.2015.12.095.

[63]   Li Z, Zhang Y, Su Y, Ouyang P, Ge J, Liu Z. Spatial co-localization of multi-enzymes by inorganic nanocrystal-protein complexes. Chem Commun 2014;50:12465–8. https://doi.org/10.1039/c4cc05478d.

[64]   Zhu YQ, Hsu WK, Grobert N, Terrones M, Terrones H, Kroto HW, et al. Self-assembly of Si nanostructures. Chem Phys Lett 2000;322:312–20. https://doi.org/10.1016/S0009-2614(00)00440-1.

[65]   Terrones M, Grobert N, Hsu WK, Zhu YQ, Hu WB, Terrones H, et al. Advances in the creation of filled nanotubes and novel nanowires. MRS Bull 1999;24:43–9. https://doi.org/10.1557/S0883769400052891.

[66]   Vaseem M, Umar A, Hahn YB, Kim DH, Lee KS, Jang JS, et al. Flower-shaped CuO nanostructures: Structural, photocatalytic and XANES studies. Catal Commun 2008;10:11–6. https://doi.org/10.1016/j.catcom.2008.07.022.

[67]   Li F, Oliva-Ramírez M, Wang D, Schaaf P. Formation and evolution of Au-SiOx Heterostructures: From nanoflowers to nanosprouts. Mater Des 2021;209:109956. https://doi.org/10.1016/j.matdes.2021.109956.

[68]   Ren Y, Xu C, Wu M, Niu M, Fang Y. Controlled synthesis of gold nanoflowers assisted by poly(vinyl pyrrolidone)-sodium dodecyl sulfate aggregations. Colloids Surfaces A Physicochem Eng Asp 2011;380:222–8. https://doi.org/10.1016/j.colsurfa.2011.02.029.

[69]   Saito G, Hosokai S, Akiyama T. Synthesis of ZnO nanoflowers by solution plasma. Mater Chem Phys 2011;130:79–83. https://doi.org/10.1016/j.matchemphys.2011.05.084.

[70]   Jia W, Su L, Lei Y. Pt nanoflower/polyaniline composite nanofibers based urea biosensor. Biosens Bioelectron 2011;30:158–64. https://doi.org/10.1016/j.bios.2011.09.006.

[71]   Kim KH, Jeong JM, Lee SJ, Choi BG, Lee KG. Protein-directed assembly of cobalt phosphate hybrid nanoflowers. J Colloid Interface Sci 2016;484:44–50. https://doi.org/10.1016/j.jcis.2016.08.059.

[72]   Wang X, Hu C, Liu H, Du G, He X, Xi Y. Synthesis of CuO nanostructures and their application for nonenzymatic glucose sensing. Sensors Actuators, B Chem 2010;144:220–5. https://doi.org/10.1016/j.snb.2009.09.067.

[73]   Thandavan K, Gandhi S, Sethuraman S, Rayappan JBB, Krishnan UM. A novel nano-interfaced superoxide biosensor. Sensors Actuators, B Chem 2013;176:884–92. https://doi.org/10.1016/j.snb.2012.09.031.

[74]   Rulíšek L, Vondrášek J. Coordination geometries of selected transition metal ions (Co2+, Ni2+, Cu2+, Zn2+, Cd2+, and Hg2+) in metalloproteins. J Inorg Biochem 1998;71:115–27. https://doi.org/10.1016/S0162-0134(98)10042-9.

[75] Hao M, Fan G, Zhang Y, Xin Y, Zhang L. Preparation and characterization of copper-Brevibacterium cholesterol oxidase hybrid nanoflowers. Int J Biol Macromol 2019;126:539–48. https://doi.org/10.1016/j.ijbiomac.2018.12.237.

[76] Ke C, Fan Y, Chen Y, Xu L, Yan Y. A new lipase-inorganic hybrid nanoflower with enhanced enzyme activity. RSC Adv 2016;6:19413–6. https://doi.org/10.1039/c6ra01564f.

[77] Jiang W, Wang X, Yang J, Han H, Li Q, Tang J. Lipase-inorganic hybrid nanoflower constructed through biomimetic mineralization: A new support for biodiesel synthesis. J Colloid Interface Sci 2018;514:102–7. https://doi.org/10.1016/j.jcis.2017.12.025.

[78] Batule BS, Park KS, Kim M Il, Park HG. Ultrafast sonochemical synthesis of protein-inorganic nanoflowers. Int J Nanomedicine 2015;10:137–42. https://doi.org/10.2147/IJN.S90274.

[79] Chung M, Nguyen TL, Tran TQN, Yoon HH, Kim IT, Kim M Il. Ultrarapid sonochemical synthesis of enzyme-incorporated copper nanoflowers and their application to mediatorless glucose biofuel cell. Appl Surf Sci 2018;429:203–9. https://doi.org/10.1016/j.apsusc.2017.06.242.

[80] Lee SW, Cheon SA, Kim M Il, Park TJ. Organic–inorganic hybrid nanoflowers: types, characteristics, and future prospects. J Nanobiotechnology 2015;13:54. https://doi.org/10.1186/s12951-015-0118-0.

[81] Gulmez C, Altinkaynak C, Özdemir N, Atakisi O. Proteinase K hybrid nanoflowers (P-hNFs) as a novel nanobiocatalytic detergent additive. Int J Biol Macromol 2018;119:803–10. https://doi.org/10.1016/j.ijbiomac.2018.07.195.

[82] Bilal M, Asgher M, Shah SZH, Iqbal HMN. Engineering enzyme-coupled hybrid nanoflowers: The quest for optimum performance to meet biocatalytic challenges and opportunities. Int J Biol Macromol 2019;135:677–90. https://doi.org/10.1016/j.ijbiomac.2019.05.206.

[83] Cipolatti EP, Silva MJA, Klein M, Feddern V, Feltes MMC, Oliveira JV, et al. Current status and trends in enzymatic nanoimmobilization. J Mol Catal B Enzym 2014;99:56–67. https://doi.org/10.1016/j.molcatb.2013.10.019.

[84] Zhang L, Ma Y, Wang C, Wang Z, Chen X, Li M, et al. Application of dual-enzyme nanoflower in the epoxidation of alkenes. Process Biochem 2018;74:103–7. https://doi.org/10.1016/j.procbio.2018.08.029.

[85] Patel SKS, Otari S V., Chan Kang Y, Lee JK. Protein-inorganic hybrid system for efficient his-tagged enzymes immobilization and its application in l-xylulose production. RSC Adv 2017;7:3488–94. https://doi.org/10.1039/c6ra24404a.

[86] Altinkaynak C, Tavlasoglu S, Kalin R, Sadeghian N, Ozdemir H, Ocsoy I, et al. A hierarchical assembly of flower-like hybrid Turkish black radish peroxidase-Cu2+ nanobiocatalyst and its effective use in dye decolorization. Chemosphere 2017;182:122–8. https://doi.org/10.1016/j.chemosphere.2017.05.012.

[87] Altinkaynak C, Kocazorbaz E, Özdemir N, Zihnioglu F. Egg white hybrid nanoflower (EW-hNF) with biomimetic polyphenol oxidase reactivity: Synthesis, characterization and potential use in decolorization of synthetic dyes. Int J Biol Macromol

2018;109:205–11. https://doi.org/10.1016/j.ijbiomac.2017.12.072.

[88]   Luo M, Li M, Jiang S, Shao H, Razal J, Wang D, et al. Supported growth of inorganic-organic nanoflowers on 3D hierarchically porous nanofibrous membrane for enhanced enzymatic water treatment. J Hazard Mater 2020;381:120947. https://doi.org/10.1016/j.jhazmat.2019.120947.

[89]   Fu M, Xing J, Ge Z. Preparation of laccase-loaded magnetic nanoflowers and their recycling for efficient degradation of bisphenol A. Sci Total Environ 2019;651:2857–65. https://doi.org/10.1016/j.scitotenv.2018.10.145.

[90]   Lin Z, Xiao Y, Wang L, Yin Y, Zheng J, Yang H, et al. Facile synthesis of enzyme-inorganic hybrid nanoflowers and their application as an immobilized trypsin reactor for highly efficient protein digestion. RSC Adv 2014;4:13888–91. https://doi.org/10.1039/c4ra00268g.

[91]   Feng N, Zhang H, Li Y, Liu Y, Xu L, Wang Y, et al. A novel catalytic material for hydrolyzing cow's milk allergenic proteins: Papain-Cu3(PO4)2·3H2O-magnetic nanoflowers. Food Chem 2020;311. https://doi.org/10.1016/j.foodchem.2019.125911.

[92]   Memon AH, Ding R, Yuan Q, Wei Y, Liang H. Facile synthesis of alcalase-inorganic hybrid nanoflowers used for soy protein isolate hydrolysis to improve its functional properties. Food Chem 2019;289:568–74. https://doi.org/10.1016/j.foodchem.2019.03.096.

[93]   Talens-Perales D, Fabra MJ, Martínez-Argente L, Marín-Navarro J, Polaina J. Recyclable thermophilic hybrid protein-inorganic nanoflowers for the hydrolysis of milk lactose. Int J Biol Macromol 2020;151:602–8. https://doi.org/10.1016/j.ijbiomac.2020.02.115.

[94]   Sun J, Ge J, Liu W, Lan M, Zhang H, Wang P, et al. Multi-enzyme co-embedded organic-inorganic hybrid nanoflowers: Synthesis and application as a colorimetric sensor. Nanoscale 2014;6:255–62. https://doi.org/10.1039/c3nr04425d.

[95]   Ariza-Avidad M, Salinas-Castillo A, Capitán-Vallvey LF. A 3D μPAD based on a multi-enzyme organic-inorganic hybrid nanoflower reactor. Biosens Bioelectron 2016;77:51–5. https://doi.org/10.1016/j.bios.2015.09.012.

[96]   Jin R, Kong D, Zhao X, Li H, Yan X, Liu F, et al. Tandem catalysis driven by enzymes directed hybrid nanoflowers for on-site ultrasensitive detection of organophosphorus pesticide. Biosens Bioelectron 2019;141:111473. https://doi.org/10.1016/j.bios.2019.111473.

[97]   Wang KY, Bu SJ, Ju CJ, Li CT, Li ZY, Han Y, et al. Hemin-incorporated nanoflowers as enzyme mimics for colorimetric detection of foodborne pathogenic bacteria. Bioorganic Med Chem Lett 2018;28:3802–7. https://doi.org/10.1016/j.bmcl.2018.07.017.

[98]   Li Y, Xie G, Qiu J, Zhou D, Gou D, Tao Y, et al. A new biosensor based on the recognition of phages and the signal amplification of organic-inorganic hybrid nanoflowers for discriminating and quantitating live pathogenic bacteria in urine. Sensors Actuators, B Chem 2018;258:803–12. https://doi.org/10.1016/j.snb.2017.11.155.

[99] Khan NR, Rathod VK. Enzyme catalyzed synthesis of cosmetic esters and its intensification: A review. Process Biochem 2015;50:1793–806. https://doi.org/10.1016/j.procbio.2015.07.014.

[100] Wang M, Nie K, Yun F, Cao H, Deng L, Wang F, et al. Biodiesel with low temperature properties: Enzymatic synthesis of fusel alcohol fatty acid ester in a solvent free system. Renew Energy 2015;83:1020–5. https://doi.org/10.1016/j.renene.2015.05.058.

[101] da Silva JRP, Nürnberg AJ, da Costa FP, Zenevicz MC, Lerin LA, Zanetti M, et al. Lipase NS40116 as catalyst for enzymatic transesterification of abdominal chicken fat as substrate. Bioresour Technol Reports 2018;4:214–7. https://doi.org/10.1016/j.biteb.2018.11.005.

[102] Betancor L, Luckarift HR. Co-immobilized coupled enzyme systems in biotechnology. Biotechnol Genet Eng Rev 2010;27:95–114. https://doi.org/10.1080/02648725.2010.10648146.

[103] Henriques RO, Bork JA, Fernandez-Lorente G, Guisan JM, Furigo A, de Oliveira D, et al. Co-immobilization of lipases and B-D-galactosidase onto magnetic nanoparticle supports: Biochemical characterization. Mol Catal 2018;453:12–21. https://doi.org/10.1016/j.mcat.2018.04.022.

[104] Janecka A, Staniszewska R, Gach K, Fichna J. Enzymatic degradation of endomorphins. Peptides 2008;29:2066–73. https://doi.org/10.1016/j.peptides.2008.07.015.

[105] Singh RL, Singh PK, Singh RP. Enzymatic decolorization and degradation of azo dyes - A review. Int Biodeterior Biodegrad 2015;104:21–31. https://doi.org/10.1016/j.ibiod.2015.04.027.

[106] Peirce S, Virgen-Ortíz JJ, Tacias-Pascacio VG, Rueda N, Bartolome-Cabrero R, Fernandez-Lopez L, et al. Development of simple protocols to solve the problems of enzyme coimmobilization. Application to coimmobilize a lipase and a β-galactosidase. RSC Adv 2016;6:61707–15. https://doi.org/10.1039/c6ra10906c.

[107] Gao L, Zhuang J, Nie L, Zhang J, Zhang Y, Gu N, et al. Intrinsic peroxidase-like activity of ferromagnetic nanoparticles. Nat Nanotechnol 2007;2:577–83. https://doi.org/10.1038/nnano.2007.260.

[108] Chen J, Andler SM, Goddard JM, Nugen SR, Rotello VM. Integrating recognition elements with nanomaterials for bacteria sensing. Chem Soc Rev 2017;46:1272–83. https://doi.org/10.1039/c6cs00313c.

[109] Liu H, Rong P, Jia H, Yang J, Dong B, Dong Q, et al. A wash-free homogeneous colorimetric immunoassay method. Theranostics 2016;6:54–64. https://doi.org/10.7150/thno.13159.

[110] Schmiemann G, Kniehl E, Gebhardt K, Matejczyk MM, Hummers-Pradier E. Diagnose des harnwegsinfekts: Eine systematische übersicht. Dtsch Arztebl 2010;107:361–7. https://doi.org/10.3238/arztebl.2010.0361.

[111] Lu X, Li Y, Du J, Zhou X, Xue Z, Liu X, et al. A novel nanocomposites sensor for epinephrine detection in the presence of uric acids and ascorbic acids. Electrochim Acta 2011;56:7261–6. https://doi.org/10.1016/j.electacta.2011.06.056.

[112] Pang Z, Hu CMJ, Fang RH, Luk BT, Gao W, Wang F, et al. Detoxification of Organophosphate Poisoning Using Nanoparticle Bioscavengers. ACS Nano 2015;9:6450–8. https://doi.org/10.1021/acsnano.5b02132.

[113] Yan X, Song Y, Zhu C, Li H, Du D, Su X, et al. MnO 2 Nanosheet-Carbon Dots Sensing Platform for Sensitive Detection of Organophosphorus Pesticides. Anal Chem 2018;90:2618–24. https://doi.org/10.1021/acs.analchem.7b04193.

[114] Michałowicz J, Duda W. Phenols - Sources and toxicity. Polish J Environ Stud 2007;16:347–62.

[115] Walker CH. Organic Pollutants: An Ecotoxicological Perspective. Second Edi. CRC Press; 2008.

[116] ECB. European Union Risk Assessment Report Phenol. 2006.

[117] Martínková L, Kotik M, Marková E, Homolka L. Biodegradation of phenolic compounds by Basidiomycota and its phenol oxidases: A review. Chemosphere 2016;149:373–82. https://doi.org/10.1016/j.chemosphere.2016.01.022.

[118] Anku WW, Mamo MA, Govender PP. Phenolic Compounds in Water: Sources, Reactivity, Toxicity and Treatment Methods. Phenolic Compd. - Nat. Sources, Importance Appl., vol. i, InTech; 2017, p. 13. https://doi.org/10.5772/66927.

[119] US Enviromental Protection Agency. Phenol Hazard Summary. Phenol 2000;1:95–108.

[120] Nadar SS, Gawas SD, Rathod VK. Self-assembled organic–inorganic hybrid glucoamylase nanoflowers with enhanced activity and stability. Int J Biol Macromol 2016;92:660–9. https://doi.org/10.1016/j.ijbiomac.2016.06.071.

[121] Altinkaynak C, Gulmez C, Atakisi O, Özdemir N. Evaluation of organic-inorganic hybrid nanoflower's enzymatic activity in the presence of different metal ions and organic solvents. Int J Biol Macromol 2020;164:162–71. https://doi.org/10.1016/j.ijbiomac.2020.07.118.

[122] Ghosh K, Balog ERM, Sista P, Williams DJ, Kelly D, Martinez JS, et al. Temperature-dependent morphology of hybrid nanoflowers from elastin-like polypeptides. APL Mater 2014;2. https://doi.org/10.1063/1.4863235.

[123] Trinder P. Determination of Glucose in Blood Using Glucose Oxidase with an Alternative Oxygen Acceptor. Ann Clin Biochem Int J Lab Med 1969;6:24–7. https://doi.org/10.1177/000456326900600108.

[124] Worthington K, Worthington V, editors. Worthington Enzyme Manual. Worthington Biochemical Corporation; 2011.

[125] Somturk B, Yilmaz I, Altinkaynak C, Karatepe A, Özdemir N, Ocsoy I. Synthesis of urease hybrid nanoflowers and their enhanced catalytic properties. Enzyme Microb Technol 2016;86:134–42. https://doi.org/10.1016/j.enzmictec.2015.09.005.

[126] Aydemir D, Gecili F, Özdemir N, Nuray Ulusu N. Synthesis and characterization of a triple enzyme-inorganic hybrid nanoflower (TrpE@ihNF) as a combination of three pancreatic digestive enzymes amylase, protease and lipase. J Biosci Bioeng 2020;129:679–86. https://doi.org/10.1016/j.jbiosc.2020.01.008.

[127] Li Y, Fei X, Liang L, Tian J, Xu L, Wang X, et al. The influence of synthesis conditions on enzymatic activity of enzyme-inorganic hybrid nanoflowers. J Mol Catal B Enzym 2016;133:92–7. https://doi.org/10.1016/j.molcatb.2016.08.001.

[128] Yu J, Wang C, Wang A, Li N, Chen X, Pei X, et al. Dual-cycle immobilization to reuse both enzyme and support by reblossoming enzyme-inorganic hybrid nanoflowers. RSC Adv 2018;8:16088–94. https://doi.org/10.1039/c8ra02051e.

[129] Koca FD, Demirezen Yilmaz D, Ertas Onmaz N, Ocsoy I. Peroxidase-like activity and antimicrobial properties of curcumin-inorganic hybrid nanostructure. Saudi J Biol Sci 2020. https://doi.org/10.1016/j.sjbs.2020.05.025.

[130] Ren W, Li Y, Wang J, Li L, Xu L, Wu Y, et al. Synthesis of magnetic nanoflower immobilized lipase and its continuous catalytic application. New J Chem 2019;43:11082–90. https://doi.org/10.1039/c8nj06429f.

[131] He G, Hu W, Li CM. Spontaneous interfacial reaction between metallic copper and PBS to form cupric phosphate nanoflower and its enzyme hybrid with enhanced activity. Colloids Surfaces B Biointerfaces 2015;135:613–8. https://doi.org/10.1016/j.colsurfb.2015.08.030.

[132] Alessi A, Agnello S, Buscarino G, Gelardi FM. Raman and IR investigation of silica nanoparticles structure. J Non Cryst Solids 2013;362:20–4. https://doi.org/10.1016/j.jnoncrysol.2012.11.006.

[133] Yu Y, Fei X, Tian J, Xu L, Wang X, Wang Y. Self-assembled enzyme-inorganic hybrid nanoflowers and their application to enzyme purification. Colloids Surfaces B Biointerfaces 2015;130:299–304. https://doi.org/10.1016/j.colsurfb.2015.04.033.

[134] Sun X, Niu H, Song J, Jiang D, Leng J, Zhuang W, et al. Preparation of a Copper Polyphosphate Kinase Hybrid Nanoflower and Its Application in ADP Regeneration from AMP. ACS Omega 2020;5:9991–8. https://doi.org/10.1021/acsomega.0c00329.

[135] Cui J, Zhao Y, Liu R, Zhong C, Jia S. Surfactant-activated lipase hybrid nanoflowers with enhanced enzymatic performance. Sci Rep 2016;6:1–13. https://doi.org/10.1038/srep27928.

[136] Cheng P, Tang M, Chen Z, Liu W, Jiang X, Pei X, et al. Dual-enzyme and NADPH co-embedded organic-inorganic hybrid nanoflowers prepared using biomimetic mineralization for the asymmetric synthesis of (: R)-(-)-pantolactone. React Chem Eng 2020;5:1973–80. https://doi.org/10.1039/d0re00158a.

[137] Chen X, Xu L, Wang A, Li H, Wang C, Pei X, et al. Efficient synthesis of the key chiral alcohol intermediate of Crizotinib using dual-enzyme@CaHPO4 hybrid nanoflowers assembled by mimetic biomineralization. J Chem Technol Biotechnol 2018;94:236–43. https://doi.org/10.1002/jctb.5769.

[138] Duan L, Li H, Zhang Y. Synthesis of Hybrid Nanoflower-Based Carbonic Anhydrase for Enhanced Biocatalytic Activity and Stability. ACS Omega 2018;3:18234–41. https://doi.org/10.1021/acsomega.8b02247.

[139] Metelitza DI, Litvinchuk A V., Savenkova MI. Peroxidase-catalyzed co-oxidation of halogen-substituted phenols and 4-aminoantipyrine. J Mol Catal 1991;67:401–11. https://doi.org/10.1016/0304-5102(91)80052-5.

[140] Zhong L, Jiao X, Hu H, Shen X, Zhao J, Feng Y, et al. Activated magnetic lipase-inorganic hybrid nanoflowers: A highly active and recyclable nanobiocatalyst for biodiesel production. Renew Energy 2021;171:825–32. https://doi.org/10.1016/j.renene.2021.02.155.